frontiers | Frontiers in Climate

TYPE Original Research
PUBLISHED 25 August 2025
DOI 10.3389/fclim.2025.1592454

OPEN ACCESS

EDITED BY
Ben W. Kolosz,
University of Hull, United Kingdom

REVIEWED BY
Martin Taylor,
University of Hull, United Kingdom
Ferdinand J. Dina Ebouel,
Botswana International University of Science and Technology, Botswana

*CORRESPONDENCE
Maria-Elena Vorrath
✉ science@mevorrath.de

RECEIVED 12 March 2025
ACCEPTED 22 July 2025
PUBLISHED 25 August 2025

CITATION
Vorrath M-E, Amann T, Meyer zu Drewer J, Hagemann N, Aldrich C, Börker J, Seedtke M, Becker JN, Hagens M, Eschenbach A and Hartmann J (2025) Pyrogenic carbon and carbonating minerals for carbon capture and storage (PyMiCCS) part II: organic and inorganic carbon dioxide removal in an Oxisol.
Front. Clim. 7:1592454.
doi: 10.3389/fclim.2025.1592454

Pyrogenic carbon and carbonating minerals for carbon capture and storage (PyMiCCS) part II: organic and inorganic carbon dioxide removal in an Oxisol

Maria-Elena Vorrath[1]*, Thorben Amann[1], Johannes Meyer zu Drewer[2,3,4], Nikolas Hagemann[3,4,5], Cierra Aldrich[6], Janine Börker[1], Maria Seedtke[7], Joscha N. Becker[7], Mathilde Hagens[8], Annette Eschenbach[7] and Jens Hartmann[1]

[1]Institute for Geology, University of Hamburg, Hamburg, Germany, [2]Institute for Sustainable Energy Systems, Offenburg University of Applied Sciences, Offenburg, Germany, [3]Agroscope, Zürich, Switzerland, [4]Ithaka Institute, Goldbach, Germany, [5]Ithaka Institute, Arbaz, Switzerland, [6]Terradot Soil Inc., San Francisco, CA, United States, [7]Institute of Soil Science, University of Hamburg, Hamburg, Germany, [8]Soil Chemistry Group, Wageningen University & Research, Wageningen, Netherlands

Enhanced rock weathering (ERW) and pyrogenic carbon capture and storage (PyCCS, or "biochar carbon removal") are two promising carbon dioxide removal (CDR) techniques that can contribute to soil restoration. These technologies can be combined by co-application of rock powder and biochar or by co-pyrolysis of rock powder with biomass to produce rock-enhanced (RE) biochar. In a 27-week laboratory experiment, we quantified the carbon (C) sink development of co-applications and RE-biochars produced by co-pyrolysis of basanite rock powder with either 50 or 90 wt% willow wood or 90 wt% wheat straw. Incubators featured two elevated soil pCO_2 levels (0.012 and 0.062 atm, equivalent to about 1.2 and 6.2 Vol-% CO_2) in a clay-rich, nutrient-poor Oxisol, with a simulated annual rainfall of 1,600 mm. Results showed strong initial fluxes of total alkalinity (TA), dissolved inorganic carbon (DIC), dissolved organic carbon (DOC), and major cations (Mg^{2+}, Ca^{2+}, K^+, Na^+), which decreased over time. Notably, elevated pCO_2 had minimal impact on the release of DOC but doubled the TA flux from ERW. An important observation was the impact of waterlogging on water fluxes in soil columns without biochar, which lowered the amount of leached cations from rock and biochar. We defined the carbon sink (C-Sink) to include all DIC of geogenic and biogenic origin, and pyrogenic carbon from biochar. Biogenic cations were not considered as contributing to additional CO_2 sequestration. For a soil application equivalent to application of 12 t ha^{-1}, the total net C-Sink ranged from −0.1 to 30.9 t CO_2 ha^{-1} after 27 weeks under 1.2 Vol-% CO_2. We were not able to determine a change in rock weathering rates from co-pyrolysis since biogenic and geogenic cations could not be distinguished. A 20-year forecast suggests net C-Sinks between 0.5 t and 28.7 t CO_2 ha^{-1}, driven by increased contributions from weathering, alongside a C-Sink loss of carbon due to biochar mineralization. While biochar alone generally produces a larger C-Sink, co-application with rock powder fosters soil remineralization and provides a higher permanence of the C-Sink. Additionally, biochar increases water-holding capacity, prevents waterlogging of soils and likely improves the retention of organic carbon in soils.

KEYWORDS

PyC, PyCCS, RE-biochar, biochar, enhanced weathering, CDR

Highlights

- No clear evidence of accelerated rock weathering.
- Waterlogging reduced alkalinity export but biochar addition mitigated this effect.
- Cations from biogenic and geogenic origin influence the CDR potential.
- Rock weathering and biochar offer a complementary CDR portfolio.

1 Introduction

Increasing global temperatures, soil degradation, depletion of mineral fertilizer resources, and declining soil organic carbon (SOC) stocks pose significant threats to agriculture and food security (Porkka et al., 2016; Zhao et al., 2017; Spinoni et al., 2021; Mbow et al., 2022; Shukla et al., 2022). Further, shifting precipitation patterns, the rising frequency of droughts, and extreme weather events call for an adaption of agricultural practices. To acknowledge these issues, the Intergovernmental Panel on Climate Change (IPCC) highlights the importance of implementing sustainable land management practices in food production (Mbow et al., 2022; Nabuurs et al., 2022). While current agricultural practices accounted for 13–21% of global anthropogenic greenhouse gas emissions between 2010 and 2019, cultivated soils also play an important role in climate change mitigation through carbon dioxide removal (CDR) by built-up of SOC (Babiker et al., 2022; Nabuurs et al., 2022). Additional CDR on agricultural land can be achieved by enhanced rock weathering (ERW), i.e., amending soils with rock powder to promote silicate mineral weathering and the transformation of CO_2 to bicarbonate, a form of dissolved inorganic carbon (DIC). Another approach involves pyrogenic carbon capture and storage (PyCCS), which uses pyrolysis to convert agricultural residues and other biomass to produce, among other products, biochar, that can be applied to agricultural soils (Schmidt et al., 2019). While PyCCS is already widely implemented (Smith et al., 2023), ERW lags behind in technological readiness, monitoring, reporting, and verification schemes (MRV), economic viability, and public support (Smith et al., 2024).

Co-benefits that enhance soil health and food security could improve public acceptance of CDR methods (Waring et al., 2023). Identifying synergies between CDR applications promting soil improvement and protection offers a promising path to scale PyCCS and ERW (Janssens et al., 2022). The co-application of biochar and rock powder was suggested to act synergistically, but has yet to be empirically tested (Amann and Hartmann, 2019; Hagens et al., 2023). Integrating these methods presents a unique opportunity for a multifaceted CDR strategy. Biochar can improve soil fertility, increase nutrient availability, improve water retention, promote root growth and ultimately increase yield, especially in tropical regions (Lehmann et al., 2021; Schmidt et al., 2021). Additionally, it helps to reduce environmental impacts of agriculture, such as nitrate leaching and N_2O emissions (Borchard et al., 2019), and can support soil remediation (Wang et al., 2022; Cornelissen et al., 2025). Specifically, biochar may reduce plant uptake of trace elements including lead and nickel (Peng et al., 2018; Schmidt et al., 2021). Application of rock powder increases soil pH, provides both macro- and micronutrients, depending on the composition of the rock (Beerling et al., 2018; Swoboda et al., 2022; Dupla et al., 2024) and improves soil structure (Beerling et al., 2018; Haque et al., 2020; Swoboda et al., 2022). Rock weathering reintroduces carbon into the geological cycle by transforming CO_2 into alkalinity in aquatic systems (Hartmann et al., 2013; Renforth, 2019). Further, the presence of secondary clay minerals, formed through mineral weathering, contributes to the stability and protection of both SOC (Buss et al., 2023) and the labile fractions of biochar (Yang et al., 2021) by facilitating the formation of mineral-associated organic matter by cation bridging, and aggregation (Buss et al., 2023). Combining biochar and rock powder has the potential not only to improve soil conditions but also to support the rehabilitation of degraded soils in response to rising food demand and the need for climate change adaptation (Amann and Hartmann, 2019; Janssens et al., 2022).

In recent years, carbon sinks (C-Sinks) based on PyCCS and ERW gained increasing research attention, both due to their large-scale potential and operational complexities. Enhanced rock weathering is characterized by its long-term carbon sequestration potential, with weathering rates that can be monitored through the analysis of weathering products in soil solutions (Amann and Hartmann, 2022; Kantola et al., 2023). However, robust MRV frameworks that directly quantify the C-Sink are still in development. The carbon sequestration effect of ERW may be impacted by the interaction of soil biota with minerals and SOC (Vicca et al., 2022), potential organic carbon (C_{org}) loss due to pH increases (Yan et al., 2023), and the influence of non-carbonic acids in the weathering process (Kantola et al., 2023). Pyrogenic carbon capture and storage involves CO_2 capture by photosynthesis and long-term sequestration by converting biomass into biochar (Rathnayake et al., 2024). If applied to soil, biochar will undergo partial oxidation by both biotic and abiotic processes (Pignatello et al., 2024) which leads to a loss of C at a rate largely dependent on the inert biochar properties. Biochar is a heterogeneous material consisting of a wide range of carbonaceous compounds (Keiluweit et al., 2010), which can be grouped into persistent and semi-persistent carbon fractions (Schmidt et al., 2022). Current MRV calculate the persistent (>100 or >1,000 years) portion of biochar using factors for the fraction of C_{org} that is in the range of 0.7–0.9 (Calvo Buendia et al., 2021; Etter et al., 2021; Schmidt et al., 2024).

Studies on the combination of both CDR technologies are scarce, yet several positive feedbacks have been suggested (Amann and Hartmann, 2019) such as the support of ERW through a higher water retention capacity in biochar-amended soil or the protection of biochar through minerals (Nan et al., 2022), and the increased formation of aggregates and mineral-associated organic matter (Han et al., 2020). A practical study addressing the co-application of rock powder for ERW and biochar in terms of a C-Sink and soil impact found only proportional, additive effects, instead of synergistic effects for ERW (Honvault et al., 2024). Beyond co-application, ERW and PyCCS can be combined by co-pyrolysis of biomass with rock powder, also referred to as rock-enriched

biochar (RE-biochar; Meyer zu Drewer et al., 2025). Although Meyer zu Drewer et al. (2025) could not confirm higher yield of pyrogenic carbon in RE-biochars, other studies found higher carbon yields through the addition of wood ash, potassium acetate, or rock powder (Buss et al., 2019, 2020; Mašek et al., 2019; Grafmüller et al., 2022).

Here, we test the impact of co-application and co-pyrolysis on weathering rates and effectiveness for carbon capture and storage. In addition to evaluation of CDR capabilities, this research will examine potential co-benefits of these soil amendments to an Oxisol (highly weathered and therefore nutrient-depleted tropical soil with low agricultural productivity). Oxisol soil columns were incubated and exposed to a low and high pCO_2 atmosphere representing different levels of root respiration. Various configurations of RE-biochars, rock powder and biochar co-application, and individual applications of pure biochar or pure rock powder were compared. The total C-Sink was evaluated through measurements of generated inorganic carbon (IC), providing the IC-Sink, complemented by pyrogenic carbon (PyC) from the (RE-)biochar providing the PyC-Sink.

2 Materials and methods

2.1 Rock, biochar and soil

We used wood and straw as common used biomass feedstocks for the biochar production and basanite as an already well-studied and ready-to-use rock powder available in Germany. To cover all possible configurations we produced pure biochars without rock powder (to be tested in co-application) and RE-biochars. Dry willow wood (*Salix viminalis L.*, 49.0 wt% C_{org}, 1.9 wt% ash, water content 3.6 wt%) was mixed and pelletized with some moisture but without binding additives with 0 wt%, 10 wt%, and 50 wt% basanite (Eifelgold, grain size between 0.5 µm and 250 µm, Supplementary S1, cf. e.g., Meyer zu Drewer et al., 2025). The pyrolysis was carried out at 650°C as detailed in Meyer zu Drewer et al. (2025). In the following, biochar and RE-biochars are referred to as W-P (biochar from wood pellets), 10BaW-P (pelleted with 10 wt% basanite) and 50BaW-P, respectively. Likewise, wheat straw (*Triticum aestivum L.*, 47.2 wt% C_{org}, 5.0 wt% ash, water content 11.2 wt%) was homogenized, pelleted with some moisture and pyrolyzed with 0 wt% (S-P) and 10 wt% basanite (10BaS-P). The biochars were analyzed by Eurofins Umwelt Ost GmbH, Germany, following the guidelines of the European Biochar Certificate (EBC, 2024). The mass conversion, rock and biogenic content, and the molar ratio of hydrogen to C_{org} (H/C_{org}) of the (RE-) biochars are presented in Table 1. More details on the analyses and calculations can be found in Supplementary S2 and in Meyer zu Drewer et al. (2025).

The relict Oxisol used for this study was collected in the area of Lich, Germany. The grain size analysis classified this soil as a clayey loam (according to the classification through the Food and Agriculture Organization of the United Nations, FAO, 2006). Prior to the experiment the soil was oven-dried and sieved to < 2 mm. A basic characterization is provided in Table 2 (method description in Supplementary S3).

2.2 Experimental setup

For the incubation experiment, acrylic tubes (length: 25 cm, inner diameter: 5.6 cm) were sealed with a 5 µm mesh plankton net at the bottom and used as downflow soil columns. For each column, 500 g of soil was homogenized with a biochar/rock powder mixture, RE-biochar or rock powder at a dose equivalent to a rock powder amendment of 40 t ha^{-1} (Table 3). In single and co-application treatments biochar was also applied with 40 t ha^{-1}. All treatments were set-up in duplicate.

The (RE-)biochars were not washed before the deployment and contained an easily soluble ash fraction. The columns were installed vertically in two incubators and, before starting the experiment, each column was saturated with 200 mL of deionized water. The incubators were then sealed and flushed with a $N_2 + CO_2$ gas mixture, resulting in CO_2 concentrations of 1.24 ± 0.47% and 6.18 ± 1.18%, respectively (calculated with PhreeqC from pH, DIC, and major ions in water, Parkhurst and Appelo, 2013; database: phreeqc.dat), due to gas leaks of the incubators (Supplementary S5). During the experiment, the columns were watered from the top with

TABLE 2 Basic soil properties including pH in H_2O and in $CaCl_2$, electrical conductivity in H_2O (EC), total carbon (C_{tot}), total inorganic carbon (TIC), organic carbon (C_{org}), total nitrogen (N_{tot}), the ratio of organic carbon to nitrogen (C_{org}/N), the effective cation exchange capacity (CEC_{eff}), the base saturation, water content (WC), water holding capacity (WHC), and particle size distribution.

Parameter	Unit	Value	Parameter	Unit	Value
pH in H_2O		6.8	CECeff	mmolc kg^{-1}	140.6
pH in $CaCl_2$		6.0	Base saturation	%	97.2
EC	µS cm^{-1}	48.3	WC	%	2.2
C_{tot}	wt%	1.84	WHC	%	64.3
TIC	wt%	0.04	Sand	wt%	19.3
C_{org}	wt%	1.80	Silt	wt%	38.1
N_{tot}	wt%	0.2	Clay	wt%	42.6
C_{org}/N		9.9			

TABLE 1 Mass conversion, rock content, biochar content and the molar ratio of hydrogen to organic carbon (H/C_{org}) in (rock enhanced) biochars produced from wood (W) or straw (S) with 10 or 50% basanite (Ba) added to the biomass prior to pelleting and pyrolysis.

Parameter		10BaW-P	50BaW-P	10BaS-P	W-P	S-P
Mass conversion	%	28.0	59.5	32.7	21.8	24.4
Rock Content	wt%	31.0	79.9	31.0	0.0	0.0
Biochar content	wt%	69.0	20.1	69.0	100	100
H/C_{org} Molar ratio		0.2	0.4	0.2	0.2	0.2

TABLE 3 Soil amendments of co-pyrolysed RE-biochar, co-applied rock powder and biochar, and single amendments normalized to 40 t ha^{-1} application of basanite. Due to differences in mass yield (section 2.1), the amendment mass per 500 g soil in each column is specified. The C-Sink potential per hectare and per tonne of material of amendment are given as a total and separated by inorganic and pyrogenic carbon (IC-SinkC-Sink from rock powder and PyC-SinkC-Sink from biochar). For the calculation of C-Sinks see chapter 2.4 and Supplementary S4.

		Co-pyrolysis			Co-application		Single application		
Column material		RE-biochar Wood with 10% Basanite	RE-biochar Wood with 50% Basanite	RE-biochar Straw with 10% Basanite	Wood biochar co-applied with Basanite	Straw biochar co-applied with Basanite	Wood biochar	Straw biochar	Basanite
Label		10BaW-P	50BaW-P	10BaS-P	W-P + Ba	S-P + Ba	W-P	S-P	Ba
Soil amendment	g per column	27.1	11.9	25.7	10.0 and 9.9	10.0 and 9.9	10	10	9.9
C-Sink potential per hectare									
Total C-Sink	t CO_2 ha^{-1}	176.33	22.66	150.60	143.88	126.53	126.51	109.16	17.36
IC-Sink		16.34	16.61	16.78	18.38	18.00	1.01	0.63	17.36
PyC-Sink		159.99	6.05	133.82	125.50	108.53	125.50	108.53	0.00
C-Sink potential per t of material									
Total C-Sink	t CO_2 t^{-1}	1.58	0.42	1.42	1.75	1.53	3.12	2.69	0.37
IC-Sink		0.13	0.29	0.14	0.20	0.19	0.03	0.02	0.37
PyC-Sink		1.45	0.13	1.28	1.55	1.34	3.09	2.67	0.00

deionized water that was sparged with N_2 + 1.5% CO_2 and N_2 + 15% CO_2 for 5 to 15 min, respectively, to pre-equilibrate the irrigation water with the simulated soil atmosphere in the incubators. The columns were watered three times a week, with 25.25 mL pre-equilibrated deionized water corresponding to rainfall of 1,600 mm $year^{-1}$. The leachate was captured in 250 mL polyethylene bottles. The experiment ran for 27 weeks at 21.3 ± 1.8°C in a dark room (Supplementary S5) without the addition of any seeds, plant material or living organisms. Gas was replenished after every watering.

2.3 Leachate analysis

At each sampling time, dissolved inorganic carbon (DIC) was sampled directly inside the incubators to prevent re-equilibration with the lab atmosphere. Outside the incubator, pH, temperature, and electrical conductivity of the leachate were immediately measured with a WTW 3630 IDS Multimeter. The sampling procedure and analyses of DIC, total alkalinity (TA, by titration), major ions (by ion chromatography), dissolved organic carbon (DOC), and dissolved silica (DSi, by colorimetric method) followed Amann et al. (2022) and are described in Supplementary S6.

2.4 Quantifications and extrapolations

As suggested by Manning et al. (2024), C-Sinks of all materials were separated into IC-Sink and PyC-Sink, due to their different behavior in soil. Additionally, we considered potential gains and losses of C over time and space to account for the actual C-Sink. TA is usually used to distinguish carbon fluxes from rock weathering, because it is the result of acid consumption in the leachate water when neutralizing alkaline substances. This includes inorganic compounds (here predominantly HCO_3^-, CO_3^{2-}, and OH^-) and organic compounds (Iticha et al., 2024; Rieder et al., n.d.). To avoid the accounting of organic acids, whose conjugate bases affect the titrated TA and likely originate from the soil, biochar, and RE-biochar, we calculated the inorganic TA based on measured DIC, pH, and cation concentrations using PhreeqC (Parkhurst and Appelo, 2013; database: phreeqc.dat) as TA_{calc}. Finally, we applied a factor for CO_2 loss due to re-equilibration in rivers and the ocean, assuming that 1 mol of TA_{calc} equals 0.85 mol of CO_2 permanently sequestered (Renforth, 2019, see Supplementary S4, equations 2, 3). We did not consider the uptake of nutrients from plants, as the experiment was conducted without plants and in the dark (Dietzen and Rosing, 2023). It is important to note that biochar also contributes to TA_{calc} through cation release from carbonates, which creates a mixed IC-Sink signal (Supplementary S4, equations 4, 5). We argue that biogenic cations released from biochar would have also been released in terms of a decomposition of the biomass, which makes their contribution to TA and CO_2 sequestration non-additional and thus this TA is not considered CDR. Therefore, the produced TA_{calc} is part of the IC-Sink, but cannot completely be accounted for as a removal of anthropogenic CO_2 and does not contribute to CDR, just like soil-released cations. For amendments which contained both rock powder as biochar, we quantified the actual CDR from TA_{calc} as a "potential CDR" ranging from minimum to maximum (e.g., 0 to 1 t CO_2 ha^{-1}) as we could not disaggregate the contribution of geogenic and biogenic cations from each material. For enhanced comparability between the treatments, we normalized all values to an application rate of 12 t ha^{-1} of a given material.

For the PyC-Sink, the C_{org} content of the initially applied (RE-) biochars was accounted for. To account for the loss of labile C_{org} from the soil and determine the remaining C_{org} fraction from PyC over time (C_{remain}), we used a conservative calculation from the most recent approach employed in the voluntary carbon market certification schemes for PyC with a H/C_{org} ratio of < 0.40 (Schmidt et al., 2024; Supplementary S7). This conservative calculation prevents an overestimation of the PyC-Sink and might be higher.

For the measured DOC, we assumed that a lower flux of DOC compared to the control column implies an enhanced retention of C_{org} from SOC, which could otherwise have been leached or respired. This retention can be considered as avoided emissions, potentially due to SOC stabilization.

The chemical fluxes were determined according to Amann et al. (2020), which is detailed in Supplementary S8. Our calculated basanite weathering rates based on leachate water (Supplementary S8) likely underestimated the actual weathering, since cations from rock weathering follow different pathways in the soil (e.g., signal retardation due to CEC), and only a fraction of them appears in soil leachate (Te Pas et al., 2025). Therefore, we instead consider the production rate of leachate TA_{calc} per mass material to be the TA that is exported from the upper soil profile of the nearfield zone as described in the Voluntary Carbon Market Standard by Cascade Climate (Mills et al., 2024). For the extrapolation of the C-Sink development over a period of 20 years we decided against a linear extrapolation as used by Vienne et al. (2024) but selected three scenarios: (1) minimum, (2) medium and (3) maximum assumed C-Sink. For the minimum C-Sink scenario, we used an exponential model fit to the last three sampling dates (week 15, 21 and 27, fit parameters in Supplementary S9) when the nutrient leaching showed a stable decrease rate. The medium C-Sink scenario was based on a decrease rate of 0.5% per week from the last sampling date (week 27), and the maximum C-Sink scenario considers the value of the last sampling date as a steady state (Supplementary S9).

2.5 Farmer-focused application scenario

We designed a farmer-focused application scenario to show how (RE-)biochar and rock powder could be combined in agriculture and what level of CDR this approach can deliver. We consider a universal lime spreader (e.g., Kurier–K 14000, Kuxmann, Bielefeld, Germany) with a carrying capacity of 12 m^3, and maximum payload of 12 t, respectively, so that the filling of the spreader will be limited either by the total volume or by the mass of the materials. The scenarios assume the spreading of RE-biochar and biochar in pelletized form, as used in this study, as well as loose rock powder for co-applications and the application of untreated rock power. We also assumed that the spreader distributes this content over 1 ha, as more frequent refilling would be too laborious.

3 Results

3.1 Observed water fluxes

At the beginning of the experiment water infiltrated quickly after watering. However, over the course of the experiment (> week 12), waterlogging occurred in 26 of 36 soil columns and the intended total water flux of 2,045 mL over 27 weeks was not achieved, i.e., less water could be added (Figure 1). The lowest water fluxes (minimum 1,168 mL) were observed in soil columns without amendment (Control) and with pure basanite powder added. The columns least affected by waterlogging contained 10BaW-P, 10BaS-P, and W-P.

3.2 Leachate chemistry

All treatments including the control column showed an increase in TA and DIC leaching during the first 9 weeks of the experiment and a slow decrease afterwards (Figure 2; Supplementary file). Except for straw-based treatments the pH values also showed a slight increase

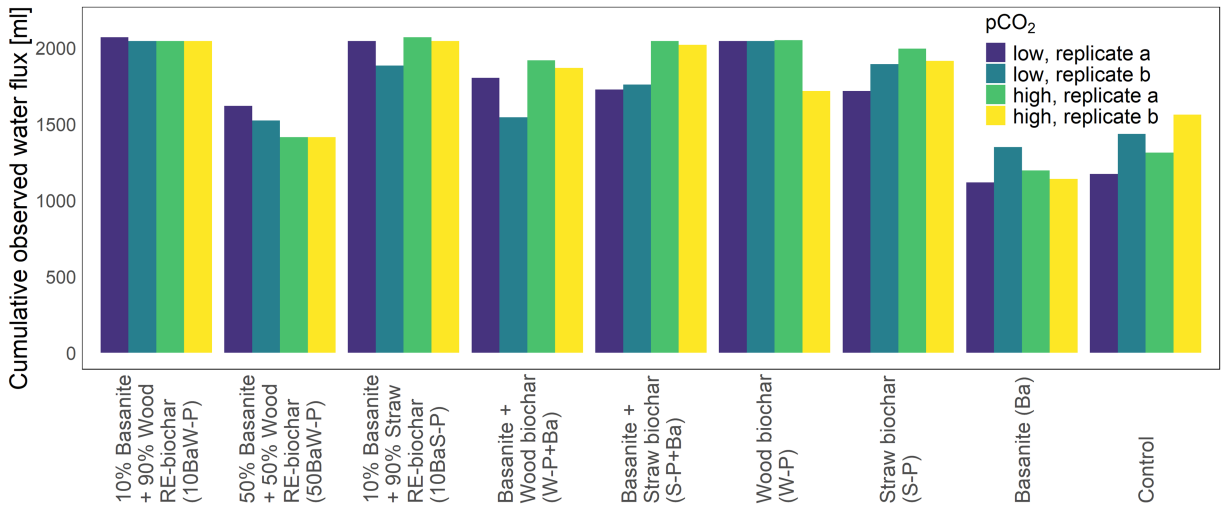

FIGURE 1
Total water fluxes from each soil column amendment with rock-enhanced (RE-)biochars, pure biochar or basanite compared to a non-amended Control (soil only) under low and high pCO_2 during 27 weeks. Water addition was planned to be 2,045 mL, but was limited by limited infiltration, i.e., waterlogging.

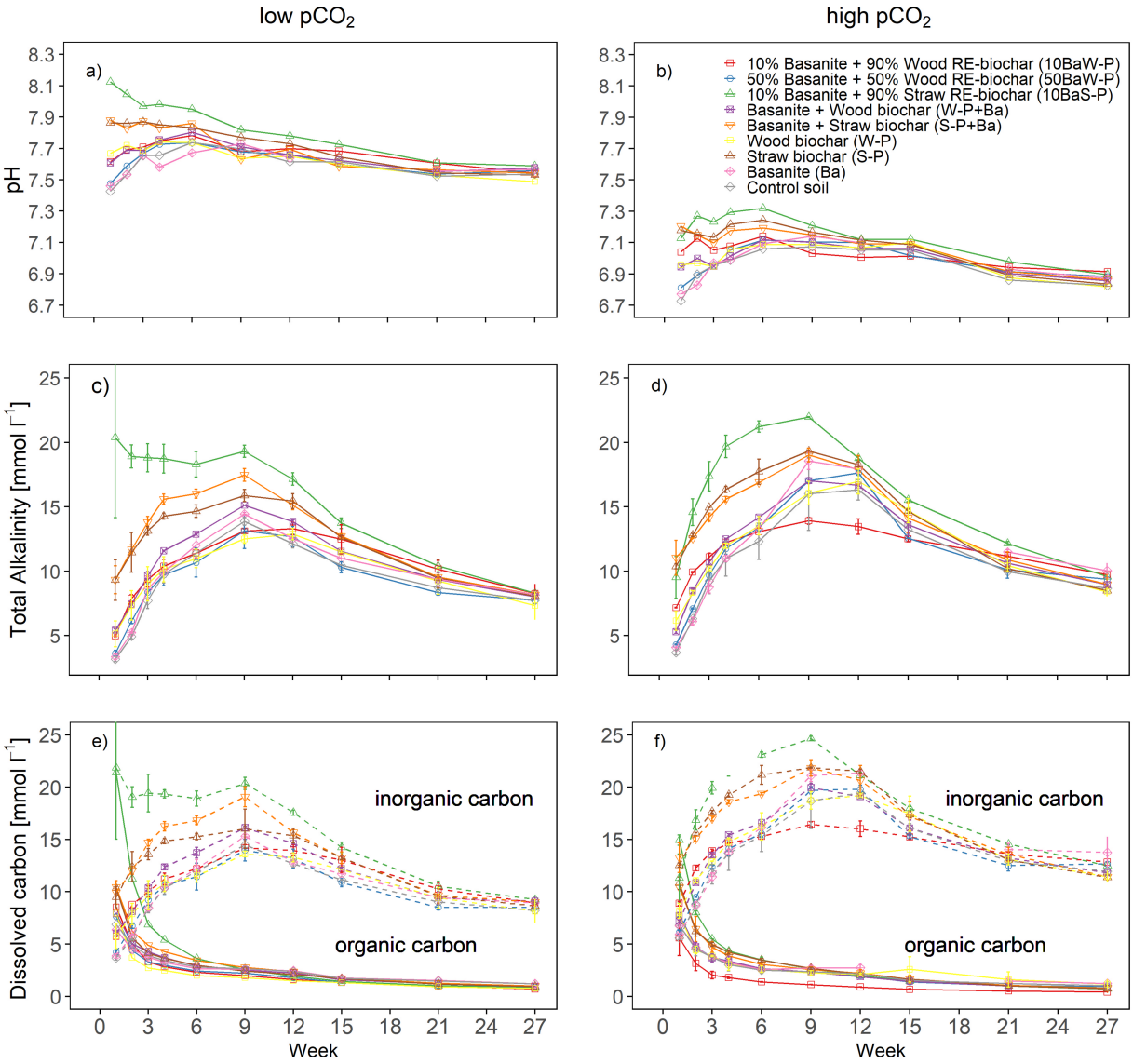

FIGURE 2
Times series data of the average bulk chemistry of leachates from column experiment with application of rock-enhanced (RE-)biochar, equivalent co-application of biochar and rockpowder and pure biochar/rock powder to an Oxisol under low (1.24%, **a**, **c**, **e**) and high (6.18%, **b**, **d**, **f**) pCO_2. The development of pH **(a,b)**, TA **(c,d)**, and concentrations of DIC and DOC **(e,f)**. Whiskers indicate the standard deviation.

until week 6 followed by a decrease. The concentration of DOC continuously decreased over time. In general, (RE-)biochar produced from straw showed higher fluxes of ions, DIC, and DOC as well as higher pH values compared to their wood-based counterparts. The pH of the leachates started with average values of 7.68 and 6.97 in the first week to 7.55 and 6.86 in week 27 for low and high pCO_2, respectively. Average TA values under low pCO_2 started with 7.12 ± 5.38 mmol kg^{-1} for all treatments, peaked at a maximum values of 24.8 mmol kg^{-1} (for 10BaS-P in week 9) and decreased to 7.98 ± 0.46 mmol kg^{-1} toward the end, again for all treatments. Under high pCO_2 average TA values started with 6.85 ± 2.73 mmol kg^{-1} increased to 17.66 ± 2.33 mmol kg^{-1} in week 9 and ended with 9.14 ± 0.61 mmol kg^{-1}. Average DIC values were 7.84 ± 5.65 mmol kg^{-1} (low pCO_2) and 8.78 ± 2.84 mmol kg^{-1} (high pCO_2) at the beginning and 8.76 ± 0.51 mmol kg^{-1} (low pCO_2) and 12.20 ± 0.87 mmol kg^{-1} (high pCO_2) at the end of the experiment. Average DOC values showed a sharp decline in the first 9 weeks and decreased overall from 9.72 ± 4.33 mmol kg^{-1} (low pCO_2) and 8.73 ± 2.79 mmol kg^{-1} (high pCO_2) down to 0.95 ± 0.19 mmol kg^{-1} (low pCO_2) and 0.87 ± 0.28 mmol kg^{-1} (high pCO_2) after 27 weeks.

The concentrations of dissolved cations varied, with values for Na^+ ranging from average 2.14 ± 3.70 mmol L^{-1} (low pCO_2, with an exceptional peak of 13.79 mmol L^{-1} from 10BaS-P), and 1.61 ± 2.02 mmol L^{-1} (high pCO_2) during the first week, and decreasing to 0.24 ± 0.20 mmol L^{-1} (low pCO_2) and 0.25 ± 0.21 mmol L^{-1} (high pCO_2) thereafter (Figure 3). The K^+ concentrations during the first week were 4.94 ± 5.17 mmol L^{-1} (low pCO_2) and 4.29 ± 3.08 mmol L^{-1} (high pCO_2), decreasing to 1.65 ± 0.51 mmol L^{-1} (low pCO_2) and 1.81 ± 0.63 mmol L^{-1} (high pCO_2) by the end of the study. For Ca^{2+}, the initial concentrations were 2.12 ± 0.50 mmol L^{-1} (low pCO_2) and 2.27 ± 0.51 mmol L^{-1} (high

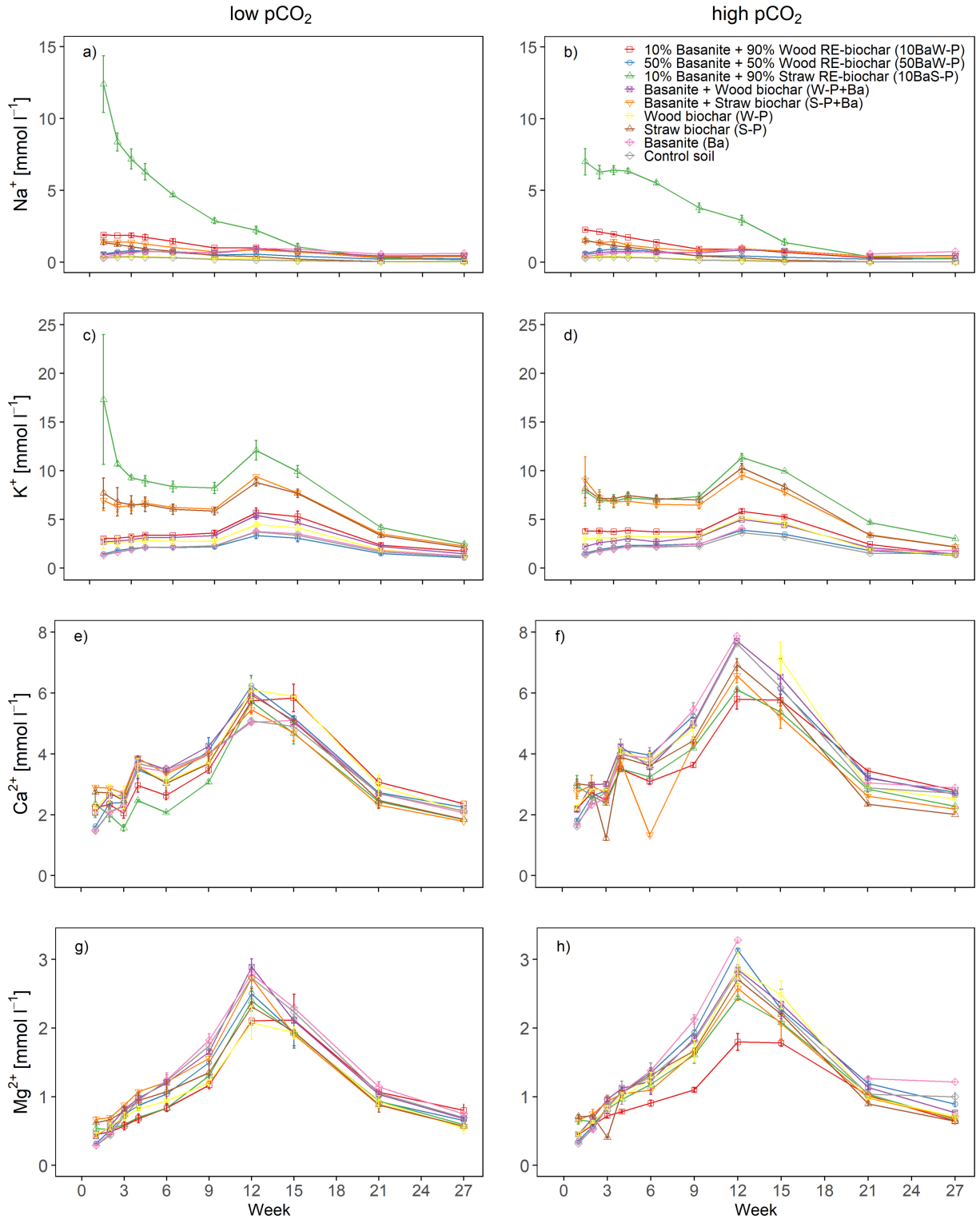

FIGURE 3
Time series data of average cation concentrations of leachates from the column experiment with application of rock-enhanced (RE) biochar, equivalent co-application of biochar and rock powder, application of pure biochar/rock powder to an Oxisol. The concentrations of sodium (Na^+) under **(a)** low pCO_2 and **(b)** high pCO_2, potassium (K^+) under **(c)** low and **(d)** high pCO_2, calcium (Ca^{2+}) under **(e)** low and **(f)** high pCO_2, and magnesium (Mg^{2+}) under **(g)** low and **(h)** high pCO_2 are shown. Whiskers indicate the standard deviation.

pCO_2), while in week 27 they remained on a similar level ranging from 2.06 ± 0.21 mmol L^{-1} (low pCO_2) to 2.51 ± 0.61 mmol L^{-1} (high pCO_2). The concentrations of Mg^{2+} were found to be 0.45 ± 0.13 mmol L^{-1} (low pCO_2) and 0.49 ± 0.14 mmol L^{-1} (high pCO_2) initially, increasing to 0.65 ± 0.09 mmol L^{-1} (low pCO_2) and 0.78 ± 0.23 mmol L^{-1} (high pCO_2) later on (Figure 3). All cation

concentrations, except for Na^+, reached their highest levels during week 12 of the experiment. Anions and DSi exhibited a consistent decline over time (see Supplementary S10). Ion concentrations did not show any impacts from waterlogging in soil columns.

3.3 Alkalinity production rate

The production of total net carbonate alkalinity TA_{prod} ranged from −80.0 µmol g^{-1} $week^{-1}$ to 360.8 µmol g^{-1} $week^{-1}$ (Figure 4). Negative values for Ba, Ba+W-P, 10BaW-P and 50BaW-P occurred when the fluxes of TA_{calc} were below the fluxes of the control soil. Toward the end, RE-biochars with 10% basanite (10BaW-P and 10BaS-P) showed the highest TA_{prod}.

3.4 DOC leaching

All amendments that contained straw (RE-)biochar showed a release of DOC equivalent to up to 1.3 mmol ha^{-1} (Figure 5). Meanwhile the applications of woody RE-biochar, wood biochar and basanite had a positive effect retaining up to 618 µmol ha^{-1} of DOC in the soil. Elevated atmospheric pCO_2 tended to decrease the DOC retention in soil columns with pure biochars, straw RE-biochar and basanite, yet increased the DOC retention for woody RE-biochar.

3.5 Total net C-Sink produced in the experiment

The cumulative TA_{calc} produced from basanite contributed to the IC-Sink in a range between −0.10 and 0.01 tCO_2 ha^{-1} under low and high pCO_2, respectively (Figure 6a). Negative alkalinity means that a given treatment TA_{calc} was lower than TA_{calc} of the control (e.g., Ba under high pCO_2). All other amendments containing biochar or RE-biochar contributed up to 0.38 tCO_2 ha^{-1} (S-P) under low pCO_2 and up to 0.42 tCO_2 ha^{-1} (S-P) under high pCO_2 (Figure 6a) to the IC-Sink, including biogenic and geogenic cations. Biochar carbon content after 27 weeks was estimated to 83.3 and 72.0% for W-P and S-P respectively, i.e., 16.7 and 28.0% of the initial carbon was lost (Supplementary S11). Therefore, the PyC-Sink ranged between 1.25 (50BaW-P) and 30.90 (W-P) tCO_2 ha^{-1} under both pCO_2 environments (Figure 6b). The total C-Sink achieved after 27 weeks ranged between 1.25 (50BaW-P) and 31.2 t CO_2 ha^{-1} (W-P) for amendments containing PyC or RE-biochar (Supplementary S12). The differences between low and high pCO_2 environments were negligible, as only impacted by changes in (relatively small) IC-Sink being affected by pCO_2. The lowest C-Sinks occurred in single basanite applications (−0.10 to 0.01 t CO_2 ha^{-1}). Further details in Supplementary S12.

During the experiment, the planned simulated rain of 1,600 mm $year^{-1}$ could not be maintained in all soil columns due to waterlogging, which directly influenced the IC-Sink would have delivered higher and positive IC-Sinks for Ba and a lower range of potential IC-Sinks from biochar and RE-biochar amendments (more details see Supplementary S12).

3.6 Net C-Sink from IC and PyC extrapolated over 20 years

The net CO_2 fluxes extrapolated over 20 years, including both the measured data and extrapolations, present the net PyC-Sink and the three IC-Sinks across the minimum, medium, and maximum scenarios (Figure 7). The IC-Sink for basanite was 0.36 and 2.54 t CO_2 ha^{-1} under low and high pCO_2 in the minimum scenario, 0.48 to 1.06 tCO_2 ha^{-1} under low and high pCO_2 in the medium scenario, and 1.82 to 4.01 tCO_2 ha^{-1} under low and high pCO_2 in the minimum scenario (Figures 7a,b). The range of possible IC-Sinks from amendments containing biochar and RE-biochar ranged from −0.31 to 0.96 under low pCO_2 (W-P and BA+W-P) and from −1.03 to 1.74 under high pCO_2 (W-P and

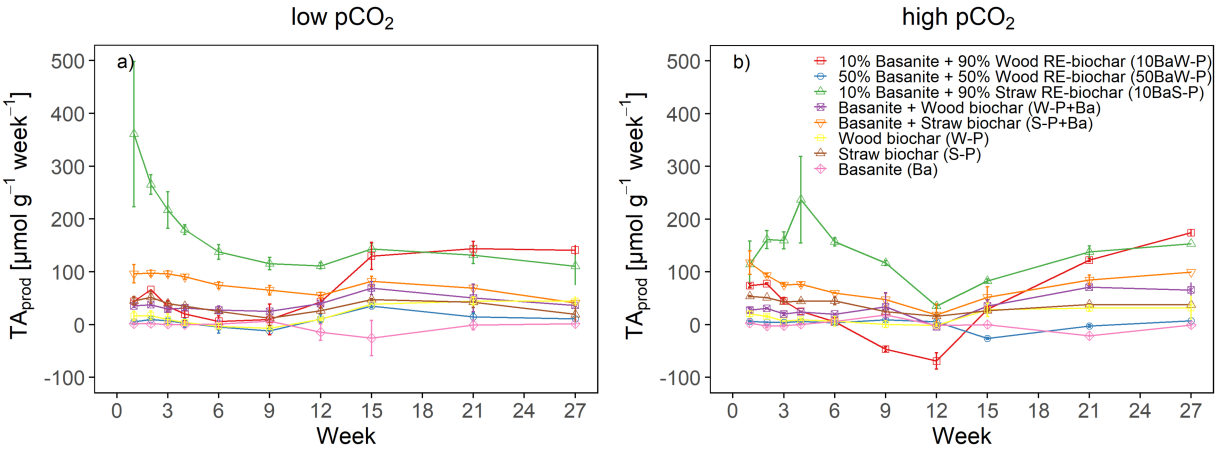

FIGURE 4
Time series data of average net total carbonate alkalinity production TA_{prod} of leachates from the column experiment with application of rock-enhanced (RE) biochar, equivalent co-application of biochar and rock powder, application of biochar and rock powder only to an Oxisol under **(a)** low and **(b)** high pCO_2. Whiskers indicate the standard deviation.

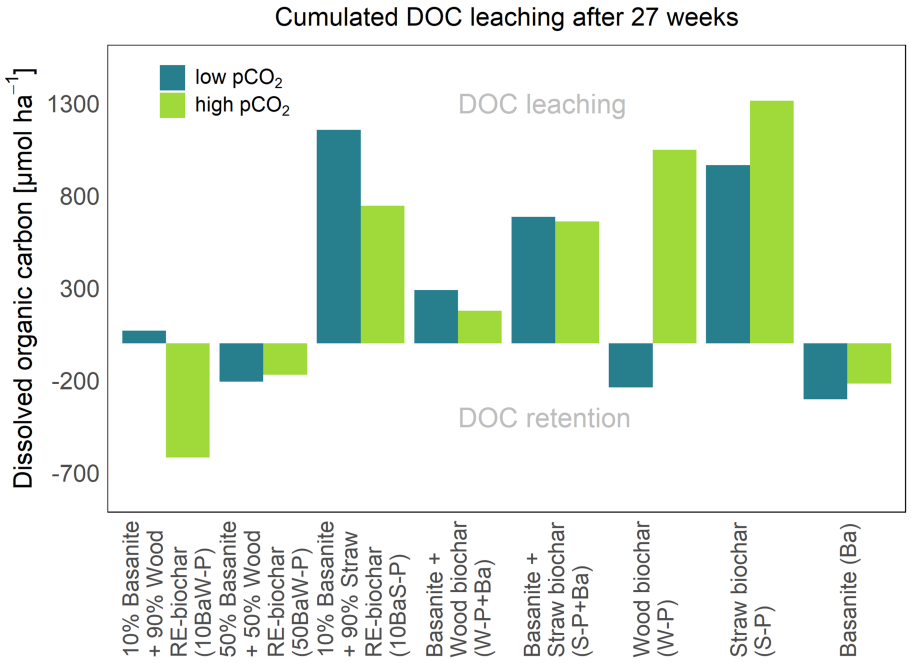

FIGURE 5
The average net loss and retention of DOC from the column experiment compared to the control with application of rock-enhanced (RE) biochar, equivalent co-application of biochar and rock powder, application of pure biochar/rock powder to an Oxisol. A positive value is associated with a loss, the negative values are associated with a retention which can be treated as avoided emissions while a DOC leaching might result in a respiration of CO_2. All values are normalized to a 12 t ha^{-1} application rate of amendment.

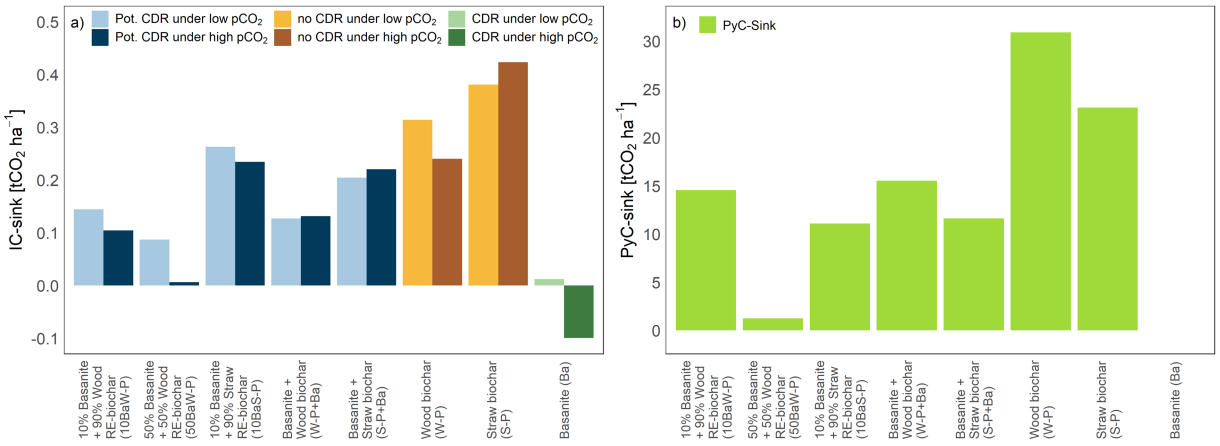

FIGURE 6
The average IC-Sinks based on leachate water and PyC-Sinks following conservative calculations as proposed in the Schmidt et al. (2024) from the column experiment with application of rock-enhanced (RE) biochar, equivalent co-application of biochar and rock powder, application of pure biochar/rock powder to an Oxisol. **(a)** The IC-Sink under low and high pCO_2 after the experiment period of 27 weeks indicating IC-Sinks with a potential contribution to CDR (blue colors) for RE-biochar and co-applications, no contribution to CDR (brown colors) for biochars and actual CDR (green colors) for basanite only application. **(b)** The PyC-Sink from all soil columns which is independent of pCO_2. Positive C-Sink values indicate negative CO_2 emissions (C sequestration) while negative C-Sink values mean positive CO_2 emissions. All values are normalized to a 12 t ha^{-1} application rate of the amendment.

50BaW-P) in all scenarios. For some treatments, extrapolations of the IC-Sinks resulted in medium scenarios lower than the minimum scenario (low pCO_2 50BaW-P, W-P, high pCO_2 10BaW-P, 50BaW-P, Ba). Remaining carbon from PyC after 20 years was 77.4% of W-P and 66.9% of S-P. The PyC-Sinks therefore ranged between 1.17 (50BaW-P) and 28.77 tCO_2 ha^{-1} (W-P; Figure 7c). The total net C-Sink (sum of experimental and extrapolated IC- and PyC-Sinks) was 0.49 (Ba) - 28.70 tCO_2 ha^{-1} (W-P) under low pCO_2 and 0.98 (Ba) - 28.70 tCO_2 ha^{-1} (W-P) under high pCO_2 (Figure 7c; Table 4).

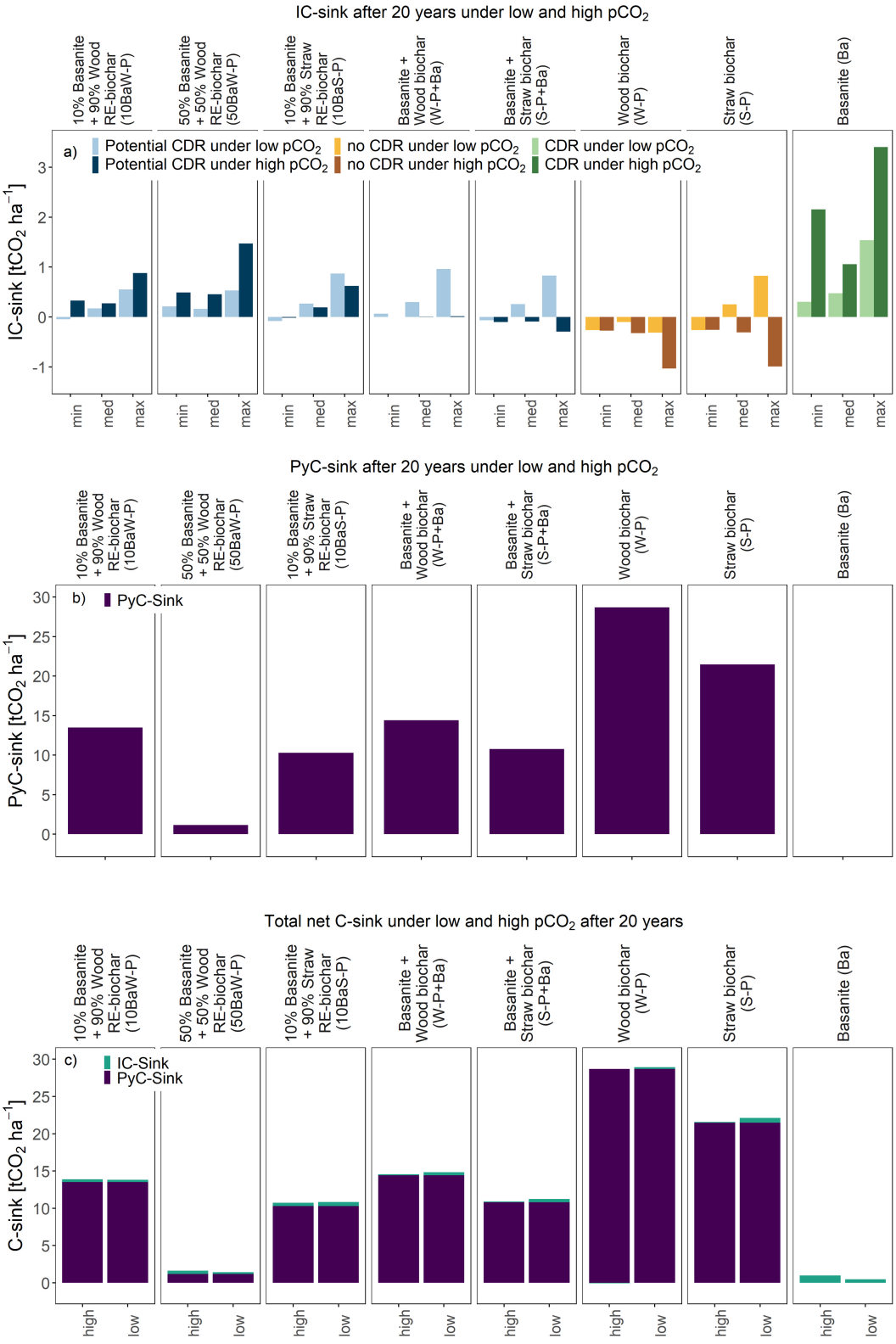

FIGURE 7
The extrapolated C-Sinks after 20 years from the column experiment with application of rock-enhanced (RE) biochar, equivalent co-application of biochar and rock powder, application of pure biochar/rock powder to an Oxisol. The IC-Sinks under **(a)** low and high pCO_2 are derived from leachate water and extrapolated as a minimum, medium and maximum scenario. **(b)** Extrapolated PyC-Sinks under low and high pCO_2 20 years after deployment are calculated after Schmidt et al. (2024). **(c)** The total net C-Sink over 20 years combined from the modeled PyC-Sink, the measured IC-Sink extrapolated following the medium scenario described above. All values are normalized to a 12 t ha^{-1} material application.

TABLE 4 The total C-Sinks after 20 years based on experimental and extrapolated data of the medium scenario. The C-Sink includes the PyC-Sink and the IC-Sink with all biogenic and geogenic cations depending on pCO_2 environment. The lowest and highest values are indicated in bold.

Amendment	C-Sink potential	PyC-Sink	IC-Sink		Total C-Sink	
			low CO_2	high CO_2	low CO_2	high CO_2
	t CO_2, application rate 12 t ha^{-1}	t CO_2 after 20 years, application rate 12 t ha^{-1}	t CO_2 after 20 years, application rate 12 t ha^{-1}		t CO_2 after 20 years, application rate 12 t ha^{-1}	
10BaW-P	18.82	13.50	0.32	0.38	13.82	13.88
50BaW-P	5.02	1.16	0.25	0.46	1.41	1.62
10BaS-P	16.75	10.29	0.53	0.43	10.83	10.72
W-P + Ba	20.83	14.42	0.43	0.14	14.85	14.56
S-P + Ba	18.31	10.78	0.46	0.13	11.25	10.91
W-P	37.09	28.70	0.22	−0.08	**28.92**	28.62
S-P	32.08	21.46	0.64	0.12	22.10	21.58
Ba	4.40	-	0.49	0.96	**0.49**	0.96

4 Discussion

4.1 Impact of soil amendments on alkalinity production and the inorganic carbon sink

Downflow column experiments have already shown a marked CDR effect from rock powder weathering in different soils (e.g., Amann et al., 2022; Te Pas et al., 2023). In our experiment, we observed an increase of pH, TA and DIC in the first 3 months, followed by a decrease. Such pattern in chemical fluxes is likely related to the CEC value of our Oxisol and the retardation of base cations in the exchangable pool by strong binding soil surfaces (Te Pas et al., 2025). Measured TA concentrations were above the control (Figure 2), however, the IC-Sink by basanite under high pCO_2 was lower compared to the control column (Figure 6a), meaning that a negative C-Sink was generated, and less CO_2 was sequestered than in the control. Although TA concentrations in leachate of Ba were higher than the control, the total TA export from the soil column to the nearfield zone was below the control due to reduced water flux. A notable challenge during the experiments was the severe clogging of pores and consecutive waterlogging toward the end, most prominent in both the control and Ba columns (Figure 1) and directly impacting the magnitude of IC-Sink. Meanwhile, addition of biochar and RE-biochar improved drainage of the columns. We assume that the waterlogging was partially due to the absence of bioturbation and roots (Shi et al., 2021); additionally, the soil had a clay content of 42.6%, which was increased to 43.7% by rock powder addition, evoking higher water impermeability. Given that hydrology is crucial for ERW and the IC-Sink, it is important to recognize that lab-based studies give limited insights into the weathering behavior in the field due to the absence of multiple biological and climatic factors. Still, our basanite soil columns are a good example an unfavorable combination of rock powder and soil impacting physical properties of the soil (Dupla et al., 2024; Te Pas et al., 2025), which illustrates the loss of the IC-Sink through a deterioration of the hydrological properties when mixing rock powder to clay-rich soils. Further, it underscores the need for careful evaluation of experimental setups for CDR laboratory studies and field applications. Moreover, the observed waterlogging demonstrates possible limitations for rock powder application in clay soils but also highlights the potential opportunities presented by biochar addition. By comparing the IC-Sink based on the simulated target precipitation of 1,600 mm $year^{-1}$, the Ba treatment resulted in a positive IC-Sink, indicating a CDR of 0.04 and 0.12 t ha^{-1} that could have been achieved under low and high pCO_2 conditions during the 27 weeks of the experiment, respectively (Supplementary S12). This range accounts for approximately 11–42% of the CDR achieved in a mesocosm experiment after 1 year by Kelland et al. (2020), which utilized Sorghum and basalt at an application rate of 12 t ha^{-1}. Therefore, it is imperative to recognize that the IC-Sink is influenced not just by the material itself, but also by the soil properties that affect water drainage; a careful assessment of soil grain size and rock feedstock grain size is required. If the grain size of rock powder and soil grain size distribution are not coordinated and waterlogging occurs, the IC-Sink will be low or even negative.

Another possible cause for the waterlogging in Ba-treated soil columns could be the increased formation of secondary minerals, resulting from a higher weathering rate associated with a higher pCO_2 (Amann et al., 2020). Still, the increased formation of secondary minerals reported in Amann et al. (2022) occurred at 100% CO_2, while CO_2 levels in our experiments were approximately 12–80 times lower. Interestingly, our study found that the IC-Sinks were not consistently elevated at higher pCO_2, despite earlier observations that suggested elevated CO_2 enhances dissolution rates (Amann et al., 2022). The lowest C-Sinks produced in Ba treatment are not just attributed to the reduced water drainage but also to its significantly lower CDR efficiency per ton of material compared to biochar/RE-biochar. The effect of CO_2 on weathering seems to be more prominent for pure minerals than in the case of co-applied biochar or RE-biochar. One reason for a lower IC-Sink based on lower TA concentrations might be an inhibited water-mineral interaction and lower weathering rates due to the pyrogenic coating of mineral grains with secondary char during co-pyrolysis as reported by Meyer zu Drewer et al. (2025). Additionally, the CDR potential per mass-unit rock is relatively low at 0.37 tCO_2 t^{-1} compared to pure biochar, which presents the equivalent of 3.12 tCO_2 t^{-1} W-P and 2.69 tCO_2 t^{-1} S-P (Table 3).

In addition to possible formation of secondary minerals within the soil columns, we observed the formation of precipitates when leachate samples were stored for several days or longer, as calcite is oversaturated in the outflow water in all treatments for most of the time (Supplementary S13). Calculated weathering rates based on the leachate cations are in a range of 10^{-10} to 10^{-12} mol m^{-2} s^{-1} (Supplementary S14), commonly observed for different ultramafic and mafic rock powders (see references in table 8 in Vienne et al., 2024) and we anticipate that in-situ weathering rates will be higher, possibly closer to rates of 10^{-6} mol m^{-2} s^{-1} as found by Brantley (2008). The parameter of the actual TA production per mass-unit of material shows stablizing rates in the last 6 weeks of the experiment with an average of 140 µmol g^{-1} $week^{-1}$ (from 10BaW-P and 10BaS-P; Figure 4). We suppose the increase and stabilization in TA to be influenced by a delay of cation release from the soil columns (Figure 2; Te Pas et al., 2025) or a delay of carbonate weathering from PyC because water infiltration into the PyC pellets may need several weeks to months.

Cation fluxes from columns treated with biochar or RE-biochar generally exceeded those from columns with Ba amendments. This may be linked to the presence of a small fraction of IC in our biochar which is up to 1.4 wt%, slightly higher than averages reported for biochars (Yuan et al., 2011; Fidel et al., 2017). Inorganic carbon in biochar is present as carbonate minerals, which dissolve much faster than silicate minerals (Brantley, 2008), this may explain the pronounced differences in TA and DIC between RE-biochar treatments compared to soil amended with rock powder only (Figure 6a). It also explains the absence of a decline of both TA production rates and weathering rates (based on the leachate water) toward the end of the experiment. This is a strong indicator that longer experiment durations would be necessary to disentangle the weathering signal of PyC-bound (carbonate-)minerals from the signal of rock dust in combined applications. Only then, a conclusive statement about effects on the weathering rate of rock powder through co-pyrolysis with biomass could be made. Future studies should consider an (acid) washing pretreatment of RE-biochar prior to the incubation experiment to avoid weathering signals from biogenic carbonates within the material.

It is crucial to recognize that while all cations contribute to the IC-Sink, not all IC-Sinks facilitate CDR. Geogenic cations released by rock weathering create additional alkalinity and with that reincorporate carbon into the long-term cycle, whereas biogenic cations released from biomass and biochar originate from soil. They would have been (re-)emitted during biomass decomposition and do not represent additional CO_2 sequestration, as these cations contributed to the alkalinity in soil before being removed by the plant. The leachate from soil columns containing RE-biochar and biochar mixed with rock powder presents a composite of cations, complicating the distinction between geogenic and biogenic sources (Figure 6a). Therefore, the assessment of CDR according to experimental performance must be approached with caution.

From a broader perspective, the combination of soil amendments shows that co-application or co-pyrolysis with biochar enhances the TA production but not automatically CDR. So far, results from co-pyrolyzed RE-biochar suggest that thermal treatment does not affect the susceptibility to weathering, with median rates comparable to those of untreated rock and PyC mixes.

4.2 The carbon sink contribution from organic carbon species

The soil application of biochar, which is an established agricultural method (Glaser et al., 2024), has developed into a globally relevant CDR technique with sequestration estimates between 0.3 and 6.6 Gt CO_{2e} $year^{-1}$ (Smith et al., 2023). While previous soil column experiments on PyC have mainly focussed on studying metal retention (e.g., Sun et al., 2020; Sun et al., 2022), nutrient leaching (e.g., Ding et al., 2010), impacts on SOC dynamics (Mukherjee and Zimmerman, 2013; Mukherjee et al., 2014), and soil hydrology (e.g., Barnes et al., 2014; Verheijen et al., 2019), there is only a small number of systematic assessments regarding the CDR potential and stability over time.

Due to its carbon content, the biochars used in this study had a potential PyC-Sink of 3.12 tCO_2 t^{-1} for W-P and 2.67 tCO_2 t^{-1} for S-P (Figure 6b; Table 3), of which > 99% is composed of C_{org}. The quality and longevity of PyC storage is highly dependent on biomass feedstocks and pyrolysis procedure and typically verified by independent certification schemes such as the Global Biochar C-Sink (Schmidt et al., 2024). Hydropyrolysis, a form of analytical pyroysis aiming to quantify the persistent fraction of the PyC (Meredith et al., 2012; Howell et al., 2022) revealed that > 90% of the C_{org} in our amendments can be defined as persistent aromatic carbon (Meyer zu Drewer et al., 2025). Persistent aromatic carbon consists of clusters containing > 7 fused aromatic rings, which are considered to be highly stable in the environment (Schmidt et al., 2022). Therefore, this part can be certified as a 1,000 years C-Sink within the voluntary carbon market (Schmidt et al., 2024).

In general, the loss of DOC from soil columns is a known phenomenon from soil rewetting as a response of microbial activity and the resulting Birch-Effect (Jarvis et al., 2007; Dong et al., 2021), regardless of the addition of soil amendments. Thus, DOC release after the addition of (RE-)biochar could equally be attributed to DOC release from the biochars, but can also be the result of influencing microbial degradation processes in the soil (priming) and thus stem from SOC. If the measured net carbon loss through DOC leaching would remain from PyC from biochar in 10BaS-P as well as in all single and co-applications of biochar (Figure 5), the loss of C_{org} was less than 0.1% of their total C_{org}, which aligns with findings from other studies (Liu et al., 2015). This DOC loss was lower than the calculated C_{org} decay rates of PyC, which were 16.7% for W-P and 28.0% for S-P of C_{org} in 27 weeks according to Schmidt et al. (2024). The clearly lower observed DOC loss compared to the estimated decay rates can be attributed to DOC leaching but the majority of PyC loss may have occurred through mineralization to CO_2. Even though this process was not measured in our experimental design, it aligns with established incubation experiments that assess C_{org} loss via CO_2 outgassing (Leng et al., 2019).

The initial loss of DOC is particularly notable in all straw-based amendments, while co-applied or co-pyrolyzed W-P amendments display a rapid onset of DOC retention (Figure 5). However, the leaching of DOC does not appear to be a long-term phenomenon, as the high concentrations of DOC were primarily observed during the first 2 months of the experiment (Figures 2e,f). This observation matches with other studies where most of the soluble C_{org} loss in a column experiment occurred during the initial flushing event (Schiedung et al., 2020). After week 9, DOC leaching of amended soils decreased and were below or equal to those of the control soil. A

retention of DOC is present in wood biochar amendments and basanite but it is not clear if this carbon will contribute to the SOC pool or will be mineralized as it was observed where the soil pH was increased in consequence of ERW (Yan et al., 2023). To decrease uncertainties, we consider retained DOC as avoided CO_2 emissions and do not count them toward a C-Sink but rather as an additional benefit for a potential SOC buildup or stabilization. In the long term, the presence of PyC and mineral particles from rock powder may stimulate the formation of mineral-associated organic matter (Buss et al., 2024) and larger aggregates (Han et al., 2020). The retention of DOC, as well as processes that enhance the build-up of SOC and/or the stability of PyC in an Oxisol (Fang et al., 2014)—such as negative priming (Lu et al., 2014), have not been assessed in this study, but could further impact the total C-Sink budget.

Consequently, while the increased stabilization of SOC may lead to reduced conversion into CO_2, it is crucial to recognize that stimulated DOC leaching may arise from enhanced microbial activity promting the decay of soil organic matter. This microbial stimulation does not necessarily hinder organic carbon stabilization; rather, it can enhance nutrient availability, fostering greater root growth and subsequent organic carbon inputs from plant materials. Studies highlight a potential long-term buildup of organic carbon in soil (Blanco-Canqui et al., 2020) though results are not universally consistent, as shown in other studies (e.g., Gross et al., 2024). Therefore, the interplay between microbial dynamics and carbon stabilization requires careful consideration in soil management practices.

4.3 A 20-year perspective on the total C-sink: building a CDR portfolio

When evaluating the total C-Sink, it is essential to consider not only the carbon fluxes from inorganic and organic sources but also the mineralization of PyC into CO_2. Consequently, the total C-Sink is composed of three components: IC fluxes from (1) rock powder and (2) carbonates in PyC, and (3) C_{org} content from PyC (Figure 6). Since the study design does not allow to clearly differentiate between the IC-Sink contributions of PyC and basanite, it remains uncertain whether the co-application and co-pyrolysis of these materials will produce synergistic effects, i.e., enhance the rock weathering rates beyond those in basanite only applications. A recent study indicated only proportional, additive benefits of co-application, such as increased total plant biomass and improved nutrient availability for plants (Honvault et al., 2024). Another investigation found that Oxisols exhibit low mineralization rates of PyC due to the presence of pH-dependent charge of minerals (Fang et al., 2014), an effect that could be enhanced in the long term with the addition of basanite. Although we could not distinctly assess the weathering rate of the basanite in combination with PyC, we recognize the advantages of co-applied PyC and rock powder. The weathering of minerals is goverened by the interaction of CO_2 with mineral surfaces which is facilitated by soil air, rainwater, and organic matter decomposition (Deng et al., 2023). Distributing very fine-grained rock powder in clayey soils clogs its pores, as observed in our experiments, which can reduce the CO_2 transport and exchange within the soil. The addition of PyC not only creates pore space but also facilitates the drainage or retention of rainwater in fine-grained soils (Sun and Lu, 2014). Furthermore, the enhanced WHC provided by PyC may sustain weathering during drier periods. We argue that spreading fine rock powder on fine-grained soils must be carefully assessed as it may seriously impair soil hydrological properties, reduce the actual IC-Sink, and negatively impact agricultural performance, an effect that may be mitigated by the addition of PyC. By combining both methods, there is potential to rehabilitate degraded soils to achieve improved-yield, CO_2-negative agriculture (Janssens et al., 2022).

The data of our experiment plus a 20-year extrapolation leads to total net C-Sinks between 0.47 (Ba) and 28.70 (W-P) $tCO_2\ ha^{-1}$ (Figure 7; Table 4). Even with data limited to 6 months, we find that initial fluxes of cations from basanite amendment under ideal hydrological conditions would have contributed between 9.1% (low pCO_2) and 12.4% (high pCO_2) to the overall IC-Sink although just covering 2.6% of the 20 years interval (Supplementary S15). This major impact of the first 6 months after application suggests that more frequent deployments (smaller iterative applications) of rock powder could enhance the immediate IC-Sink creation. However, it is crucial to consider the deployment techniques. Regular tilling could reactivate the rock powder that may be bound to aggregates and revive its weathering potential. At the same time, disturbing the soil through tilling while adding PyC and rock powder leads to increased oxygenation of soil pore space and breakdown of aggregates, which may promote the mineralization of soil organic matter (Sekaran et al., 2021; Six et al., 2000). The effects may vary significantly depending on whether these materials are simply applied to the topsoil or integrated using less disruptive techniques, such as reduced tillage (Paustian et al., 2016). The dynamic development of the net C-Sink observed during our experiment (Figures 2e,f) highlights the importance of careful data interpretation in soil column studies. The rapid decline in IC fluxes as well as the decay of PyC indicates that CDR rates from short-term experiments may not be reliable for long-term extrapolations. Therefore, we recommend conducting long-term experiments (Paessler et al., 2025)—the longer the better—to establish dependable extrapolations and improve weathering models, as previously emphasized in other studies (e.g., Hagens et al., 2023).

Due to the calculation of PyC decay there was no difference between the low and high pCO_2, and current literature suggests that soil pH plays a minimal role in PyC decay (Rechberger et al., 2017). Although there is no direct correlation found between soil pH and biochar, acidic soils may slow down biochar decomposition. Some studies emphasize the importance of biochar properties and propose a two-pool model where the second pool of biochar is largely independent of environmental factors (Sanei et al., 2025). This complexity reflects ongoing discussions in the field, highlighting the need for further research into the environmental impacts of biochar.

A 20-year extrapolation of DOC leaching indicates a reduced leaching (except Ba and W-P under high pCO_2; Supplementary S16), and that initial leaching is followed by year-long DOC retention through SOC buildup. It is not clear how the retained DOC incorporates into present SOC stocks and how this will impact the CDR potential of this carbon species. Mechanistically, the retention of DOC is likely evoked by adsorption onto the charged surfaces of PyC (Smebye et al., 2016) or related particles, or it might involve the formation of aggregates (Bucka et al., 2019). Opposite to suggestions (Buss et al., 2024) the addition of basanite only did not increase DOC retention, as the formation of mineral-associated organic matter or

aggregates might have been diminished by the absence of roots and soil fauna (Lehmann et al., 2017; Mueller et al., 2024).

The combination of CDR methods that form additional C-Sinks on different time scales and in carbon pools was suggested to build a sustainable negative emissions portfolio (Amann and Hartmann, 2019; Rueda et al., 2021). At the time of deployment of RE-biochar, the CDR potential is primarily determined by the C_{org} fraction of the (RE-)biochar. Ultimately, the interplay between the increase in additional IC-Sink through rock weathering processes and the decrease in PyC-Sink due to mineralization may achieve a level of equilibrium in the long-term.

Depending on the fraction of basanite and PyC, such a balanced C-Sink can be achieved with higher amounts of rock dust. Assuming that the geogenic part of the IC-Sink is 50% the soil amendment 50BaW-P (Figure 8a) provides a total C-Sink of 1.3 t CO_2 ha^{-1} in year 20 which is only 0.1 t CO_2 ha^{-1} lower than at the day of its soil application. With lower basanite amounts and thus a reduced IC-Sink, the decomposition of a high PyC fraction is hardly counterbalanced like in the case of 10BaW-P (Figure 8b) where a loss of 3.8 t CO_2 ha^{-1} occurred. The effect of IC-Sink buildup from ERW balancing the carbon loss from PyC is particularly interesting for the creation of constant carbon removal portfolios over time, ensuring that losses from one C pool are headged by gains in another C pool, creating a stable and persistent C-Sink. It is important to note that a high C-Sink like 17.4 t CO_2 ha^{-1} from 10BaW-P does not automatically provide a balanced CDR portfolio. Figure 8 also indicates that long-term experiments are critical for a better understanding of the CDR of both IC and OC species over time.

4.4 A farmer-focused application scenario of RE-biochar, PyC, and basanite powder for CDR

The application doses of rock powder in numerous studies, which range from 50 to 400 t ha^{-1} (Vienne et al., 2024), are impractical for several reasons. For instance, applying 100 t rock dust per hectare would require 5–10 truckloads for transport, along with the use of large lime spreaders, resulting in considerable time and fuel consumption, as well as soil compaction, in addition to regular field work. Here, a thought experiment aims to identify an economically and technically optimized application that maximizes CDR efficiency in real-world scenarios. The CDR potential, CDR at the day of application, and CDR 20 years after application (medium scenario, low soil pCO_2) were calculated as shown in Table 5.

The application of W-P and a respective 1:1 co-application with basanite yields C-Sinks of 9.3 t CO_2 and 8.7 to 9.0 t CO_2, respectively, 20 years after the deployment of these materials into the soil (Table 5). A slightly lower C-Sink is observed with S-P and its co-application with basanite powder, achieving 6.5 t CO_2 and 6.0 to 6.3 t CO_2, respectively. The three RE-biochar configurations and the application of pure rock powder are on the lower end of CDR.

If 12 t of W-P or W-P + Ba were once applied on all agriculturally used Oxisols in the humid tropics, it would result in CDR of 1.7 Gt CO_2 and 1.6 to 1.7 Gt CO_2 after 20 years (calculations and map see Supplementary S17), respectively. This number shows the significant potential of CDR by ERW. However, the net climate benefit might be lower due to resource access, the suitability of soils (Paessler et al., 2024), the emissions in the CDR life cycle, and the costs of work force. To achieve such CDR would require 0.7 Gt of W-P or 1.3 Gt of W-P + Ba material. Feedstocks in our experiments were high-quality biomass leading to high C_{org} content in the PyC. When scaled globally, biomass of varying carbon content would likely be used for pyrolysis resulting in partly lower C_{org} content and possibly lower and less stable PyC fraction which decreases the potential C-Sink of PyC applications. Other restrictions would be the maximum amount of phosphorus that is allowed to be applied annually and might restrict the use of mineral organic phosphorus fertilizer when rock powder is used as well. These calculated C-Sinks do not account for the additional effects of this CDR method, including the benefits of higher permanence through geochemical CDR,

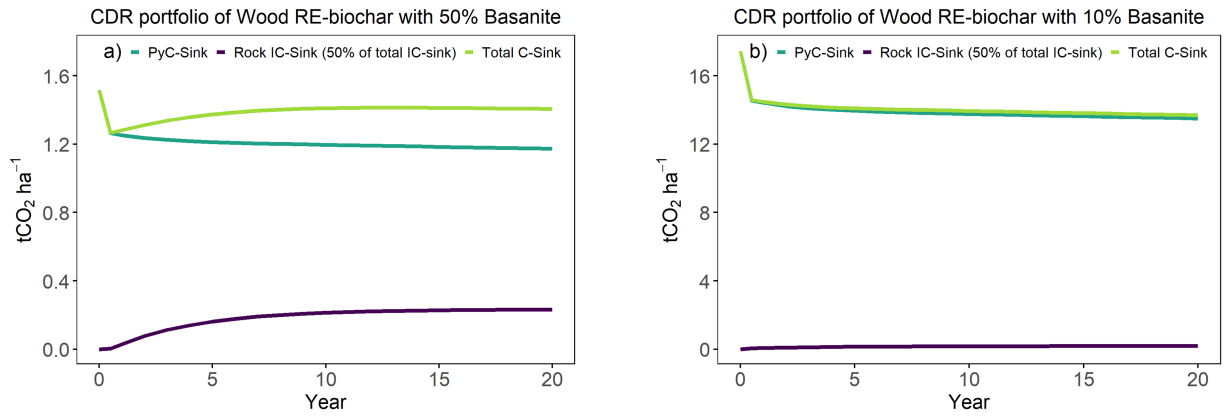

FIGURE 8
Illustration of two possible CDR portfolios showing the development of the C-Sinks of **(a)** the Wood RE-biochar with 50% basanite (50BaW-P) and **(b)** the Wood RE-biochar with 10% basanite (10BaW-P) under high pCO_2 and over 20 years. The development of the total C-Sink over time is created by the increasing IC-Sink and the decreasing PyC-Sink. We assume that 50% of the IC-Sink are geogenic and contribute to CDR. The data is combined from the 27-week experiment and extrapolated data and normalized to an application rate of 12 t ha^{-1}.

TABLE 5 Estimations of CDR in an application scenario with a lime spreader of 12 t or 12 m^3 of material, respectively. The CDR potential, the CDR on the day of application and after 20 years are considered. *limiting factor for the maximum application rate for the lime spreader which is either volume or weight. The two largest C-Sinks after 20 years are indicated in bold.

Amendment	Bulk density	Volume	Weight	CDR per t material		CDR potential	CDR on application day	CDR after 20 years
	t m^{-3}	m^3	t	CDR IC	CDR PyC	tCO_2 ha^{-1}	tCO_2 ha^{-1}	tCO_2 ha^{-1}
10BaW-P	0.336	12.00*	4.03	0–0.1	1.5	5.9–6.3	5.9	4.3–4.7
50BaW-P	0.57	12.00*	6.84	0–0.3	0.1	0.9–2.9	0.9	0.7–0.8
10BaS-P	0.324	12.00*	3.88	0–0.1	1.3	5.0–5.5	5.0	3.3–3.5
W-P + Ba	0.602	12.00*	7.22	0–0.2	1.6	11.2–12.6	11.2	**8.7–9.0**
S-P + Ba	0.557	12.00*	6.69	0–0.2	1.3	9.0–10.3	9.0	6.0–6.3
W-P	0.325	12.00*	3.9	-	3.1	12.1	12.1	**9.3**
S-P	0.301	12.00*	3.62	-	2.7	9.7	9.7	6.5
Ba	1.209	9.93	12.00*	0.4	-	4.4	0.0	0.5

improvements in soil fertility, the increase of SOC pools, the effects of minerals on PyC stabilization, the cost per ton of CDR delivered by the respective method and the socioeconomic benefits for the farmers.

For the agricultural sector utilizing PyC-based CDR, the addition of basanite may not offer a distinct advantage due to a lower mass-based C-Sink and the slow development of the IC-Sink; however, it is essential to recognize the possibility of fertilizing nutrient-poor soils with minerals, as suggested with the Rocks for Crops concept (van Straaten, 2004). In such cases, rock powder can enhance the value of PyC application at an affordable price, particularly in low-income countries with (sub-)tropical climates. Further, when pelletized or granulated together, not just dust from the spreading of rock powder can be avoided (Levy et al., 2024) but also a loss of PyC material through wind by heavier pellets. For ERW, the inclusion of PyC can significantly boost the C-Sink while ensuring improvements in hydrology (and consequently, continuous weathering), as observed in our experiments with fine-grained soils, and by utilizing local biomass in a circular manner to boost the C-Sink and avoid biomass burning. When considering the appropriate combination of both methods, access to and affordability of local resources should be prioritized as well as grain size distribution of both soil and rock powder, soil conditions, and nutrient demand of the target soil.

5 Conclusion

The interplay between inorganic and organic carbon dynamics in engineered soils highlights the complexity of scaling up durable CDR. While ERW and PyC applications have both shown promise as individual strategies, co-benefits can be created from interactions of both materials. When their biogeochemical and hydrological effects are systematically integrated, they can reinforce each other in ways that go beyond their standalone benefits.

Our findings suggest that ERW efficiency is not purely determined by mineral dissolution speed but is strongly influenced by physical soil parameters like soil texture and water movement. This means that tailored soil amendments (e.g., improving soil hydrology) are essential to optimize CDR. Biochar, actively modifies soil hydrology, likely stabilizes SOC, and can help mitigate pore-space limitations that slow down mineral weathering in compacted soils.

The temporal dynamics in the development of C-Sinks generated by different CDR technologies are of great relevance. Rock weathering delivers an initial burst of inorganic carbon fluxes, while biochar alteration occurs on longer timescales. Short-term studies often capture only the immediate weathering response, missing the longer-term equilibrium between sequestration and carbon loss. Our results indicate that ERW may require periodic re-application of rock dust to maintain stable CDR rates over time. Similarly, the long-term stability of biochar depends not only on its chemical structure but also on interactions with soils. This highlights the need for a more dynamic perspective on CDR, to account for shifting balances between transient and persistent carbon pools.

Looking ahead, integrating ERW and biochar into agricultural systems will require interdisciplinary perspectives. Predictive models need to bridge the gap between lab-derived weathering rates and real-world field conditions. Optimizing the applied materials should improve compatibility with soils while minimizing potential downsides.

Finally, there is the socio-economic dimension: Adoption by farmers will depend on whether CDR strategies align with agricultural productivity, cost efficiency, and practical feasibility. Pelletized amendments, as tested in this study, could help by reducing dust emissions and improving handling, but true scalability will depend on circular supply chains enabeling the use of local biomass and mineral resources.

To achieve gigaton-scale CDR it is crucial to look beyond individual approaches and more importantly, retrieve long-term data from field applications. By combining the geochemical carbon sink with the long-term stability of biochar, we can develop multifunctional soil amendments that support not only climate mitigation but also soil health and agricultural resilience.

Data availability statement

The original contributions presented in the study are included in the article/Supplementary material, further inquiries can be directed to the corresponding author.

Author contributions

M-EV: Conceptualization, Data curation, Formal analysis, Investigation, Methodology, Software, Validation, Visualization, Writing – original draft, Writing – review & editing. TA: Conceptualization, Data curation, Formal analysis, Funding acquisition, Investigation, Methodology, Project administration, Software, Validation, Writing – original draft, Writing – review & editing. JMzD: Investigation, Methodology, Validation, Writing – review & editing. NH: Conceptualization, Funding acquisition, Resources, Supervision, Validation, Writing – review & editing. CA: Formal analysis, Investigation, Writing – review & editing. JaB: Formal analysis, Software, Validation, Visualization, Writing – review & editing. MS: Investigation, Methodology, Writing – review & editing. JoB: Data curation, Methodology, Writing – review & editing. MH: Methodology, Supervision, Validation, Writing – review & editing. AE: Funding acquisition, Writing – review & editing. JH: Conceptualization, Funding acquisition, Project administration, Supervision, Writing – review & editing.

Funding

The author(s) declare that financial support was received for the research and/or publication of this article. This study was financed by the Federal Ministry of Research, Technology and Space (BMFTR) of the Federal Republic of Germany, grant number 01LS2109C and 01LS2109A (PyMiCCS) as part of the CDRterra research program (2022–2025).

Acknowledgments

We warmly thank our technicians Peggy Bartsch, Tom Jäppinen, Deborah Harms and Annika Naumann, and our student assistants Lennard Stoeck, and Irmak Gök. We also thank the three reviewers for their time and helpful suggestions to improve this study.

Conflict of interest

TA and CA contributed to this work prior to leaving for a private-sector role in CDR where TA is using ex-situ alkalinity reactors and CA is in the field of commercial enhanced rock weathering. This had no influence on the study.

The remaining authors declare that the research was conducted in the absence of any commercial or financial relationships that could be construed as a potential conflict of interest.

The author(s) declared that they were an editorial board member of Frontiers, at the time of submission. This had no impact on the peer review process and the final decision.

Generative AI statement

The author(s) declare that no Gen AI was used in the creation of this manuscript.

Publisher's note

Supplementary material

The Supplementary material for this article can be found online at: https://www.frontiersin.org/articles/10.3389/fclim.2025.1592454/full#supplementary-material

References

Amann, T., and Hartmann, J. (2019). Ideas and perspectives: synergies from co-deployment of negative emission technologies. *Biogeosciences* 16, 2949–2960. doi: 10.5194/bg-16-2949-2019

Amann, T., and Hartmann, J. (2022). Carbon accounting for enhanced weathering. *Front. Clim.* 4:849948. doi: 10.3389/fclim.2022.849948

Amann, T., Hartmann, J., Hellmann, R., Pedrosa, E. T., and Malik, A. (2022). Enhanced weathering potentials—the role of in situ CO2 and grain size distribution. *Front. Clim.* 4:929268. doi: 10.3389/fclim.2022.929268

Amann, T., Hartmann, J., Struyf, E., De Oliveira Garcia, W., Fischer, E. K., Janssens, I., et al. (2020). Enhanced weathering and related element fluxes – a cropland mesocosm approach. *Biogeosciences* 17, 103–119. doi: 10.5194/bg-17-103-2020

Babiker, M., Berndes, G., Blok, K., Cohen, B., Cowie, A., Geden, O., et al. (2022). "Cross-sectoral perspectives," in Climate change 2022: Mitigation of climate change. Contribution of working group III to the sixth assessment report of the intergovernmental panel on climate change, eds. P. R. Shukla, J. Skea, R. Slade, KhourdajieA. Al, DiemenR. van and D. McCollumet al. (Cambridge, UK and New York, NY, USA: Cambridge University Press), 1245–1354.

Barnes, R. T., Gallagher, M. E., Masiello, C. A., Liu, Z., and Dugan, B. (2014). Biochar-induced changes in soil hydraulic conductivity and dissolved nutrient fluxes constrained by laboratory experiments. *PLoS One* 9:e108340. doi: 10.1371/journal.pone.0108340

Beerling, D. J., Leake, J. R., Long, S. P., Scholes, J. D., Ton, J., Nelson, P. N., et al. (2018). Farming with crops and rocks to address global climate, food and soil security. *Nat Plants* 4, 138–147. doi: 10.1038/s41477-018-0108-y

Blanco-Canqui, H., Laird, D. A., Heaton, E. A., Rathke, S., and Acharya, B. S. (2020). Soil carbon increased by twice the amount of biochar carbon applied after 6 years: field evidence of negative priming. *GCB Bioenergy* 12, 240–251. doi: 10.1111/gcbb.12665

Borchard, N., Schirrmann, M., Cayuela, M. L., Kammann, C., Wrage-Mönnig, N., Estavillo, J. M., et al. (2019). Biochar, soil and land-use interactions that reduce nitrate leaching and N2O emissions: a meta-analysis. *Sci. Total Environ.* 651, 2354–2364. doi: 10.1016/j.scitotenv.2018.10.060

Brantley, S. L. (2008). "Kinetics of mineral dissolution" in Kinetics of water-rock interaction. eds. S. L. Brantley, J. D. Kubicki and A. F. White (New York, NY: Springer New York), 151–210.

Bucka, F. B., Kölbl, A., Uteau, D., Peth, S., and Kögel-Knabner, I. (2019). Organic matter input determines structure development and aggregate formation in artificial soils. *Geoderma* 354:113881. doi: 10.1016/j.geoderma.2019.113881

Buss, W., Bogush, A., Ignatyev, K., and Mašek, O. (2020). Unlocking the fertilizer potential of waste-derived biochar. *ACS Sustain. Chem. Eng.* 8, 12295–12303. doi: 10.1021/acssuschemeng.0c04336

Buss, W., Hasemer, H., Ferguson, S., and Borevitz, J. (2023). Stabilisation of soil organic matter with rock dust partially counteracted by plants. *Glob. Chang. Biol.* 30:e17052. doi: 10.1111/gcb.17052

Buss, W., Hasemer, H., Sokol, N. W., Rohling, E. J., and Borevitz, J. (2024). Applying minerals to soil to draw down atmospheric carbon dioxide through synergistic organic and inorganic pathways. *Commun. Earth Environ.* 5:602. doi: 10.1038/s43247-024-01771-3

Buss, W., Jansson, S., Wurzer, C., and Mašek, O. (2019). Synergies between BECCS and biochar—maximizing carbon sequestration potential by recycling wood ash. *ACS Sustain. Chem. Eng.* 7, 4204–4209. doi: 10.1021/acssuschemeng.8b05871

Calvo Buendia, E., Tanabe, K., Kranjc, A., Baasansuren, J., Fukuda, M., Ngarize, S., et al. (2021). 2019 refinement to the 2006 IPCC guidelines for National Greenhouse gas Inventories. Switzerland: IPCC.

Cornelissen, G., Briels, N., Bucheli, T. D., Estoppey, N., Gredelj, A., Hagemann, N., et al. (2025). A virtuous cycle of phytoremediation, pyrolysis, and biochar applications toward safe PFAS levels in soil, feed, and food. *J. Agric. Food Chem.* 73, 3283–3285. doi: 10.1021/acs.jafc.5c00651

Deng, H., Sonnenthal, E., Arora, B., Breunig, H., Brodie, E., Kleber, M., et al. (2023). The environmental controls on efficiency of enhanced rock weathering in soils. *Sci. Rep.* 13:9765. doi: 10.1038/s41598-023-36113-4

Dietzen, C., and Rosing, M. T. (2023). Quantification of CO2 uptake by enhanced weathering of silicate minerals applied to acidic soils. *Int. J. Greenhouse Gas Control* 125:103872. doi: 10.1016/j.ijggc.2023.103872

Ding, Y., Liu, Y.-X., Wu, W.-X., Shi, D.-Z., Yang, M., and Zhong, Z.-K. (2010). Evaluation of biochar effects on nitrogen retention and leaching in multi-layered soil columns. *Water Air Soil Pollut.* 213, 47–55. doi: 10.1007/s11270-010-0366-4

Dong, H., Zhang, S., Lin, J., and Zhu, B. (2021). Responses of soil microbial biomass carbon and dissolved organic carbon to drying-rewetting cycles: a meta-analysis. *Catena* 207:105610. doi: 10.1016/j.catena.2021.105610

Dupla, X., Claustre, R., Bonvin, E., Graf, I., Le Bayon, R.-C., and Grand, S. (2024). Let the dust settle: impact of enhanced rock weathering on soil biological, physical, and geochemical fertility. *Sci. Total Environ.* 954:176297. doi: 10.1016/j.scitotenv.2024.176297

EBC (2024). Guidelines for a Sustatinable production of biochar. Arbaz, Switzerland: Ithaka Institute. (Accessed February 17, 2025).

Etter, H., Vera, A., Aggarwal, C., Delaney, M., and Manley, S. (2021). Methodology for biochar utilization in soil and non-soil applications. Washington: Verra.

Fang, Y., Singh, B., Singh, B. P., and Krull, E. (2014). Biochar carbon stability in four contrasting soils. *Eur. J. Soil Sci.* 65, 60–71. doi: 10.1111/ejss.12094

FAO (2006). Guidelines for soil description. *4th* Edn. Rome: Food and Agriculture Organization of the United Nations.

Fidel, R. B., Laird, D. A., Thompson, M. L., and Lawrinenko, M. (2017). Characterization and quantification of biochar alkalinity. *Chemosphere* 167, 367–373. doi: 10.1016/j.chemosphere.2016.09.151

Glaser, B., McKey, D., Giani, L., Teixeira, W., and Schneeweiß, J. (2024). "Historical accumulation of biochar as a soil amendment" in Biochar for environmental management (eds.) J Lehmann and J Stephen. (London, New York: Routledge).

Grafmüller, J., Böhm, A., Zhuang, Y., Spahr, S., Müller, P., Otto, T. N., et al. (2022). Wood ash as an additive in biomass pyrolysis: effects on biochar yield, properties, and agricultural performance. *ACS Sustain. Chem. Eng.* 10, 2720–2729. doi: 10.1021/acssuschemeng.1c07694

Gross, A., Bromm, T., Polifka, S., Fischer, D., and Glaser, B. (2024). Long-term biochar and soil organic carbon stability – evidence from field experiments in Germany. *Sci. Total Environ.* 954:176340. doi: 10.1016/j.scitotenv.2024.176340

Hagens, M., Hartmann, J., Vicca, S., and Beerling, D. J. (2023). Editorial: enhanced weathering and synergistic combinations with other CDR methods. *Front. Clim.* 5:1244396. doi: 10.3389/fclim.2023.1244396

Han, L., Sun, K., Yang, Y., Xia, X., Li, F., Yang, Z., et al. (2020). Biochar's stability and effect on the content, composition and turnover of soil organic carbon. *Geoderma* 364:114184. doi: 10.1016/j.geoderma.2020.114184

Haque, F., Santos, R. M., and Chiang, Y. W. (2020). Optimizing inorganic carbon sequestration and crop yield with Wollastonite soil amendment in a microplot study. *Front. Plant Sci.* 11:1012. doi: 10.3389/fpls.2020.01012

Hartmann, J., West, A. J., Renforth, P., Köhler, P., De La Rocha, C. L., Wolf-Gladrow, D. A., et al. (2013). Enhanced chemical weathering as a geoengineering strategy to reduce atmospheric carbon dioxide, supply nutrients, and mitigate ocean acidification. *Rev. Geophys.* 51, 113–149. doi: 10.1002/rog.20004

Honvault, N., Tiouchichine, M.-L., Sauze, J., Piel, C., Landais, D., Devidal, S., et al. (2024). Additive effects of basalt enhanced weathering and biochar co-application on carbon sequestration, soil nutrient status and plant performance in a mesocosm experiment. *Appl. Geochem.* 169:106054. doi: 10.1016/j.apgeochem.2024.106054

Howell, A., Helmkamp, S., and Belmont, E. (2022). Stable polycyclic aromatic carbon (SPAC) formation in wildfire chars and engineered biochars. *Sci. Total Environ.* 849:157610. doi: 10.1016/j.scitotenv.2022.157610

Iticha, B., Mosley, L. M., and Marschner, P. (2024). Combining lime and organic amendments based on titratable alkalinity for efficient amelioration of acidic soils. *Soil* 10, 33–47. doi: 10.5194/soil-10-33-2024

Janssens, I. A., Roobroeck, D., Sardans, J., Obersteiner, M., Peñuelas, J., Richter, A., et al. (2022). Negative erosion and negative emissions: combining multiple land-based carbon dioxide removal techniques to rebuild fertile topsoils and enhance food production. *Front. Clim.* 4:928403. doi: 10.3389/fclim.2022.928403

Jarvis, P., Rey, A., Petsikos, C., Wingate, L., Rayment, M., Pereira, J., et al. (2007). Drying and wetting of Mediterranean soils stimulates decomposition and carbon dioxide emission: the "birch effect.". *Tree Physiol.* 27, 929–940. doi: 10.1093/treephys/27.7.929

Kantola, I. B., Blanc-Betes, E., Masters, M. D., Chang, E., Marklein, A., Moore, C. E., et al. (2023). Improved net carbon budgets in the US Midwest through direct measured impacts of enhanced weathering. *Glob. Chang. Biol.* 29, 7012–7028. doi: 10.1111/gcb.16903

Keiluweit, M., Nico, P. S., Johnson, M. G., and Kleber, M. (2010). Dynamic molecular structure of plant biomass-derived black carbon (biochar). *Environ. Sci. Technol.* 44, 1247–1253. doi: 10.1021/es9031419

Kelland, M. E., Wade, P. W., Lewis, A. L., Taylor, L. L., Sarkar, B., Andrews, M. G., et al. (2020). Increased yield and CO_2 sequestration potential with the C_4 cereal Sorghum bicolor cultivated in basaltic rock dust-amended agricultural soil. *Glob. Chang. Biol.* 26, 3658–3676. doi: 10.1111/gcb.15089

Lehmann, J., Cowie, A., Masiello, C. A., Kammann, C., Woolf, D., Amonette, J. E., et al. (2021). Biochar in climate change mitigation. *Nat. Geosci.* 14, 883–892. doi: 10.1038/s41561-021-00852-8

Lehmann, A., Zheng, W., and Rillig, M. C. (2017). Soil biota contributions to soil aggregation. *Nat Ecol Evol* 1, 1828–1835. doi: 10.1038/s41559-017-0344-y

Leng, L., Huang, H., Li, H., Li, J., and Zhou, W. (2019). Biochar stability assessment methods: a review. *Sci. Total Environ.* 647, 210–222. doi: 10.1016/j.scitotenv.2018.07.402

Levy, C. R., Almaraz, M., Beerling, D. J., Raymond, P., Reinhard, C. T., Suhrhoff, T. J., et al. (2024). Enhanced rock weathering for carbon removal–monitoring and mitigating potential environmental impacts on agricultural land. *Environ. Sci. Technol.* 58:acs.est.4c02368. doi: 10.1021/acs.est.4c02368

Liu, P., Ptacek, C. J., Blowes, D. W., Berti, W. R., and Landis, R. C. (2015). Aqueous leaching of organic acids and dissolved organic carbon from various biochars prepared at different temperatures. *J. Environ. Qual.* 44, 684–695. doi: 10.2134/jeq2014.08.0341

Lu, W., Ding, W., Zhang, J., Li, Y., Luo, J., Bolan, N., et al. (2014). Biochar suppressed the decomposition of organic carbon in a cultivated sandy loam soil: a negative priming effect. *Soil Biol. Biochem.* 76, 12–21. doi: 10.1016/j.soilbio.2014.04.029

Manning, D. A. C., De Azevedo, A. C., Zani, C. F., and Barneze, A. S. (2024). Soil carbon management and enhanced rock weathering: the separate fates of organic and inorganic carbon. *Eur. J. Soil Sci.* 75:e13534. doi: 10.1111/ejss.13534

Mašek, O., Buss, W., Brownsort, P., Rovere, M., Tagliaferro, A., Zhao, L., et al. (2019). Potassium doping increases biochar carbon sequestration potential by 45%, facilitating decoupling of carbon sequestration from soil improvement. *Sci. Rep.* 9:5514. doi: 10.1038/s41598-019-41953-0

Mbow, C., Rosenzweig, C., Barioni, L. G., Benton, T. G., and Herrero, M. (2022). "Food security" in Climate change and land: IPCC special report on climate change, desertification, land degradation, sustainable land management, food security, and greenhouse gas fluxes in terrestrial ecosystems. eds. P. R. Shukla, J. Skea, E. C. Buendia, V. Masson-Delmotte, H.-O. Pörtner and D. C. Robertset al. (US: Cambridge University Press).

Meredith, W., Ascough, P. L., Bird, M. I., Large, D. J., Snape, C. E., Sun, Y., et al. (2012). Assessment of hydropyrolysis as a method for the quantification of black carbon using standard reference materials. *Geochim. Cosmochim. Acta* 97, 131–147. doi: 10.1016/j.gca.2012.08.037

Meyer zu Drewer, J., Vorrath, M.-E., Amann, T., Hartmann, J., De la Rosa, J. M., Möllmer, J., et al. (2025). Combining pyrogenic carbon and carbonating minerals for enhanced plant growth and carbon capture and storage (PyMiCCS) part I. *Front. Clim.* 7:1631368. doi: 10.3389/fclim.2025.1631368

Mills, J. V., Sanchez, J., Olagaray, N. Y., Wang, H., and Tune, A. K. (2024). Foundations for carbon dioxide removal quantification in ERW deployments. Cascade Climate. Available online at: https://cascadeclimate.org/blog/foundations-for-carbon-removal-quantification-in-erw-deployments (Accessed February 21, 2025).

Mueller, C. W., Baumert, V., Carminati, A., Germon, A., Holz, M., Kögel-Knabner, I., et al. (2024). From rhizosphere to detritusphere – soil structure formation driven by plant roots and the interactions with soil biota. *Soil Biol. Biochem.* 193:109396. doi: 10.1016/j.soilbio.2024.109396

Mukherjee, A., Lal, R., and Zimmerman, A. R. (2014). Impacts of biochar and other amendments on soil-carbon and nitrogen stability: a laboratory column study. *Soil Sci. Soc. Am. J.* 78, 1258–1266. doi: 10.2136/sssaj2014.01.0025

Mukherjee, A., and Zimmerman, A. R. (2013). Organic carbon and nutrient release from a range of laboratory-produced biochars and biochar–soil mixtures. *Geoderma* 193-194, 122–130. doi: 10.1016/j.geoderma.2012.10.002

Nabuurs, G.-J., Mrabet, R., Abu Hatab, A., Bustamante, M., Clark, H., Havlík, P., et al. (2022). "Agriculture, forestry and other land uses (AFOLU)," in Climate change 2022: Mitigation of climate change. Contribution of working group III to the sixth assessment report of the intergovernmental panel on climate change, eds. P. R. Shukla, J. Skea, R. Slade, KhourdajieA. Al, DiemenR. van and D. McCollumet al. Cambridge, UK and New York, NY, USA: Cambridge University Press, 747–860.

Nan, H., Mašek, O., Yang, F., Xu, X., Qiu, H., Cao, X., et al. (2022). Minerals: a missing role for enhanced biochar carbon sequestration from the thermal conversion of biomass to the application in soil. *Earth Sci. Rev.* 234:104215. doi: 10.1016/j.earscirev.2022.104215

Paessler, D., Hammes, J., Smet, I., Steffens, R., Stöckel, A. A., and Hartmann, J. (2025). Learnings from running the world's largest greenhouse EW experiment. Carbon Drawdown Initiative.

Paessler, D., Steffens, R., Hammes, J., and Smet, I. (2024). Insights from monitoring leachate alkalinity, pCO_2 and CO_2 efflux of 400 weathering experiments over one year working paper-V1.0-April 11th 2024. Carbon Drawdown Initiative.

Parkhurst, D. L., and Appelo, C. A. J. (2013). "Description of input and examples for PHREEQC version 3—a computer program for speciation, batch-reaction, one-dimensional transport, and inverse geochemical calculations" in U.S. Geological Survey techniques and methods (Denver: U.S. Geological Survey), 497.

Paustian, K., Lehmann, J., Ogle, S., Reay, D., Robertson, G. P., and Smith, P. (2016). Climate-smart soils. *Nature* 532, 49–57. doi: 10.1038/nature17174

Peng, X., Deng, Y., Peng, Y., and Yue, K. (2018). Effects of biochar addition on toxic element concentrations in plants: a meta-analysis. *Sci. Total Environ.* 616-617, 970–977. doi: 10.1016/j.scitotenv.2017.10.222

Pignatello, J. J., Uchimiya, M., and Abiven, S. (2024). "Aging of biochar in soils and its implications" in Biochar for environmental management (eds.) J Lehmann and J Stephen. (Routledge).

Porkka, M., Gerten, D., Schaphoff, S., Siebert, S., and Kummu, M. (2016). Causes and trends of water scarcity in food production. *Environ. Res. Lett.* 11:015001. doi: 10.1088/1748-9326/11/1/015001

Rathnayake, D., Schmidt, H.-P., Leifeld, J., Bürge, D., Bucheli, T. D., and Hagemann, N. (2024). Quantifying soil organic carbon after biochar application: how to avoid (the risk of) counting CDR twice? *Front. Clim.* 6:1343516. doi: 10.3389/fclim.2024.1343516

Rechberger, M. V., Kloss, S., Rennhofer, H., Tintner, J., Watzinger, A., Soja, G., et al. (2017). Changes in biochar physical and chemical properties: accelerated biochar aging in an acidic soil. *Carbon* 115, 209–219. doi: 10.1016/j.carbon.2016.12.096

Renforth, P. (2019). The negative emission potential of alkaline materials. *Nat. Commun.* 10:1401. doi: 10.1038/s41467-019-09475-5

Rieder, L., Hagens, M., Poetra, R., Vidal, A., Calogiuri, T., Neubeck, A., et al. Contribution of dissolved organic carbon to total alkalinity in enhanced weathering experiments. *Appl. Geochem.* (under review).

Rueda, O., Mogollón, J. M., Tukker, A., and Scherer, L. (2021). Negative-emissions technology portfolios to meet the 1.5 °C target. *Global Environmental Change* 67:102238. doi: 10.1016/j.gloenvcha.2021.102238

Sanei, H., Petersen, H. I., Chiaramonti, D., and Masek, O. (2025). Evaluating the two-pool decay model for biochar carbon permanence. *Biochar* 7:9. doi: 10.1007/s42773-024-00408-0

Schiedung, M., Bellè, S.-L., Sigmund, G., Kalbitz, K., and Abiven, S. (2020). Vertical mobility of pyrogenic organic matter in soils: a column experiment. *Biogeosciences* 17, 6457–6474. doi: 10.5194/bg-17-6457-2020

Schmidt, H.-P., Abiven, S., and Hagemann, N. (2022). Permanence of soil applied biochar. An executive summary for global biochar carbon sink certification. *Biochar J.*, 69–74.

Schmidt, H.-P., Anca-Couce, A., Hagemann, N., Werner, C., Gerten, D., Lucht, W., et al. (2019). Pyrogenic carbon capture and storage. *GCB Bioenergy* 11, 573–591. doi: 10.1111/gcbb.12553

Schmidt, H.-P., Kammann, C., and Hagemann, N. (2024). Certification of the carbon sink potential of biochar. Available online at: http://carbon-standards.com (Accessed February 17, 2025).

Schmidt, H.-P., Kammann, C., Hagemann, N., Leifeld, J., Bucheli, T. D., Sánchez Monedero, M. A., et al. (2021). Biochar in agriculture – a systematic review of 26 global meta-analyses. *GCB Bioenergy* 13, 1708–1730. doi: 10.1111/gcbb.12889

Sekaran, U., Sagar, K. L., and Kumar, S. (2021). Soil aggregates, aggregate-associated carbon and nitrogen, and water retention as influenced by short and long-term no-till systems. *Soil and Tillage Research*. 208:104885. doi: 10.1016/j.still.2020.104885

Shi, X., Qin, T., Yan, D., Tian, F., and Wang, H. (2021). A meta-analysis on effects of root development on soil hydraulic properties. *Geoderma* 403:115363. doi: 10.1016/j.geoderma.2021.115363

Shukla, P. R., Skea, J., Calvo Buendia, E., Masson-Delmotte, V., Pörtner, H.-O., and Roberts, D. C.et al. (Eds.) (2022). Climate change and land: IPCC special report on climate change, desertification, land degradation, sustainable land management, food security, and greenhouse gas fluxes in terrestrial ecosystems. *1st* Edn. US: Cambridge University Press.

Six, J., Elliott, E. T., and Paustian, K. (2000). Soil macroaggregate turnover and microaggregate formation: a mechanism for C sequestration under no-tillage agriculture. *Soil Biology and Biochemistry.* 32, 2099–2103. doi: 10.1016/S0038-0717(00)00179-6

Smebye, A., Alling, V., Vogt, R. D., Gadmar, T. C., Mulder, J., Cornelissen, G., et al. (2016). Biochar amendment to soil changes dissolved organic matter content and composition. *Chemosphere* 142, 100–105. doi: 10.1016/j.chemosphere.2015.04.087

Smith, S. M., Fuss, S., Buck, H., Schenuit, F., Pongratz, J., Schulte, I., et al. (2024). The state of carbon dioxide removal. *2nd* Edn. Oxford: OSF.

Smith, S. M., Geden, O., Nemet, G. F., Gidden, M. J., Lamb, W. F., Powis, C., et al. (2023). The state of carbon dioxide removal. *1st* Edn. Oxford: The State of Carbon Dioxide Removal.

Spinoni, J., Barbosa, P., Cherlet, M., Forzieri, G., McCormick, N., Naumann, G., et al. (2021). How will the progressive global increase of arid areas affect population and land-use in the 21st century? *Glob. Planet. Chang.* 205:103597. doi: 10.1016/j.gloplacha.2021.103597

Sun, J., Cui, L., Quan, G., Yan, J., Wang, H., and Wu, L. (2020). Effects of biochar on heavy metals migration and fractions changes with different soil types in column experiments. *BioRes* 15, 4388–4406. doi: 10.15376/biores.15.2.4388-4406

Sun, F., and Lu, S. (2014). Biochars improve aggregate stability, water retention, and pore-space properties of clayey soil. *J. Plant Nutr. Soil Sci.* 177, 26–33. doi: 10.1002/jpln.201200639

Sun, P., Wang, Z., An, S., Zhao, J., Yan, Y., Zhang, D., et al. (2022). Biochar-supported nZVI for the removal of Cr(VI) from soil and water: advances in experimental research and engineering applications. *J. Environ. Manag.* 316:115211. doi: 10.1016/j.jenvman.2022.115211

Swoboda, P., Döring, T. F., and Hamer, M. (2022). Remineralizing soils? The agricultural usage of silicate rock powders: a review. *Sci. Total Environ.* 807:150976. doi: 10.1016/j.scitotenv.2021.150976

Te Pas, E. E. E. M., Chang, E., Marklein, A. R., Comans, R. N. J., and Hagens, M. (2025). Accounting for retarded weathering products in comparing methods for quantifying carbon dioxide removal in a short-term enhanced weathering study. *Front. Clim.* 6:1524998. doi: 10.3389/fclim.2024.1524998

Te Pas, E. E. E. M., Hagens, M., and Comans, R. N. J. (2023). Assessment of the enhanced weathering potential of different silicate minerals to improve soil quality and sequester CO2. *Front. Clim.* 4:954064. doi: 10.3389/fclim.2022.954064

van Straaten, P. (2004) Rocks for crops: Agrominerals of sub-saharan Africa Nairobi ICRAF

Verheijen, F. G. A., Zhuravel, A., Silva, F. C., Amaro, A., Ben-Hur, M., and Keizer, J. J. (2019). The influence of biochar particle size and concentration on bulk density and maximum water holding capacity of sandy vs sandy loam soil in a column experiment. *Geoderma* 347, 194–202. doi: 10.1016/j.geoderma.2019.03.044

Vicca, S., Goll, D. S., Hagens, M., Hartmann, J., Janssens, I. A., Neubeck, A., et al. (2022). Is the climate change mitigation effect of enhanced silicate weathering governed by biological processes? *Glob. Chang. Biol.* 28, 711–726. doi: 10.1111/gcb.15993

Vienne, A., Frings, P., Poblador, S., Steinwidder, L., Rijnders, J., Schoelynck, J., et al. (2024). Earthworms in an enhanced weathering mesocosm experiment: effects on soil carbon sequestration, base cation exchange and soil CO2 efflux. *Soil Biol. Biochem.* 199:109596. doi: 10.1016/j.soilbio.2024.109596

Wang, Y., Wang, H.-S., Tang, C.-S., Gu, K., and Shi, B. (2022). Remediation of heavy-metal-contaminated soils by biochar: a review. *Environ. Geotech.* 9, 135–148. doi: 10.1680/jenge.18.00091

Waring, B. G., Gurgel, A., Köberle, A. C., Paltsev, S., and Rogelj, J. (2023). Natural climate solutions must embrace multiple perspectives to ensure synergy with sustainable development. *Front. Clim.* 5:1216175. doi: 10.3389/fclim.2023.1216175

Yan, Y., Dong, X., Li, R., Zhang, Y., Yan, S., Guan, X., et al. (2023). Wollastonite addition stimulates soil organic carbon mineralization: evidences from 12 land-use types in subtropical China. *Catena* 225:107031. doi: 10.1016/j.catena.2023.107031

Yang, F., Xu, Z., Huang, Y., Tsang, D. C. W., Ok, Y. S., Zhao, L., et al. (2021). Stabilization of dissolvable biochar by soil minerals: release reduction and organo-mineral complexes formation. *J. Hazard. Mater.* 412:125213. doi: 10.1016/j.jhazmat.2021.125213

Yuan, J.-H., Xu, R.-K., and Zhang, H. (2011). The forms of alkalis in the biochar produced from crop residues at different temperatures. *Bioresour. Technol.* 102, 3488–3497. doi: 10.1016/j.biortech.2010.11.018

Zhao, C., Liu, B., Piao, S., Wang, X., Lobell, D. B., Huang, Y., et al. (2017). Temperature increase reduces global yields of major crops in four independent estimates. *Proc. Natl. Acad. Sci.* 114, 9326–9331. doi: 10.1073/pnas.1701762114